PHM for electric vehicles

PHMe 2020, 31/07/2020

Introduction

- **Abstract:** With the development of electric vehicles (EVs) in different application domains, the reliability issue is drawing increasing attention. To achieve more reliable and more durable EVs, PHM has become the concerns of both academic and industrial communities. This panel is dedicated to gathering the recent works and thoughts of PHM methods and their applications for the key components of various EVs, including different energy sources, power converters, energy storage units, and electric machines.

- **Panelists:**
  Zhenbin Zhang (Shandong University, China)
  Rui Zhao (National Research Council Canada)
  Jie Dang (GTake Electric Co. Ltd, China)
  Zhongliang Li (Aix-Marseille University, France)

Panelists

Prof. Zhenbin Zhang received the Ph.D. degree in 2016 from Technical University of Munich (TUM), Germany. Since 2017, he has been a Full Professor with Shandong University, China. Since 2018, he was appointed as a National Distinguished Expert (supported by the Youth Talent Program) of China. His research interests include power electronics and electrical drives, sustainable energy systems.

Dr. Rui Zhao is a Research Council Officer at National Research Council of Canada (NRC). Prior to joining NRC, Dr. Zhao received a Ph.D. degree from Carleton University in 2018 and worked as a postdoctoral fellow at the University of California, Berkeley. Dr. Zhao has co-authored around 25 publications and patents. His research involves lithium-ion (Li-ion) battery thermal management system, Li-ion battery failure analysis and safety design, as well as modelling and optimization of Li-ion batteries.

Dr. Jie Dang graduates from Tsinghua University China in 2009 with a bachelor degree in electrical engineering, and he got the Ph.D. in the electrical engineering at Georgia Tech USA in 2015. His research focus is on electric machine design and motor control. He is with Gtake in Shenzhen China now, with the title of VP of international business development.

Dr. Zhongliang Li received the Ph.D. degree from Aix-Marseille University, France, in 2014. Between 2014 and 2016, he worked in Fuel Cell Lab in France as postdoc. Since 2016, he has been worked as associate professor in Aix-Marseille University. His research interests concern fuel cell system analysis and optimization.

Talk 1: EV/HEV motor controller

Panelist: Dr. Jie Dang (Gtake co. ltd, China)

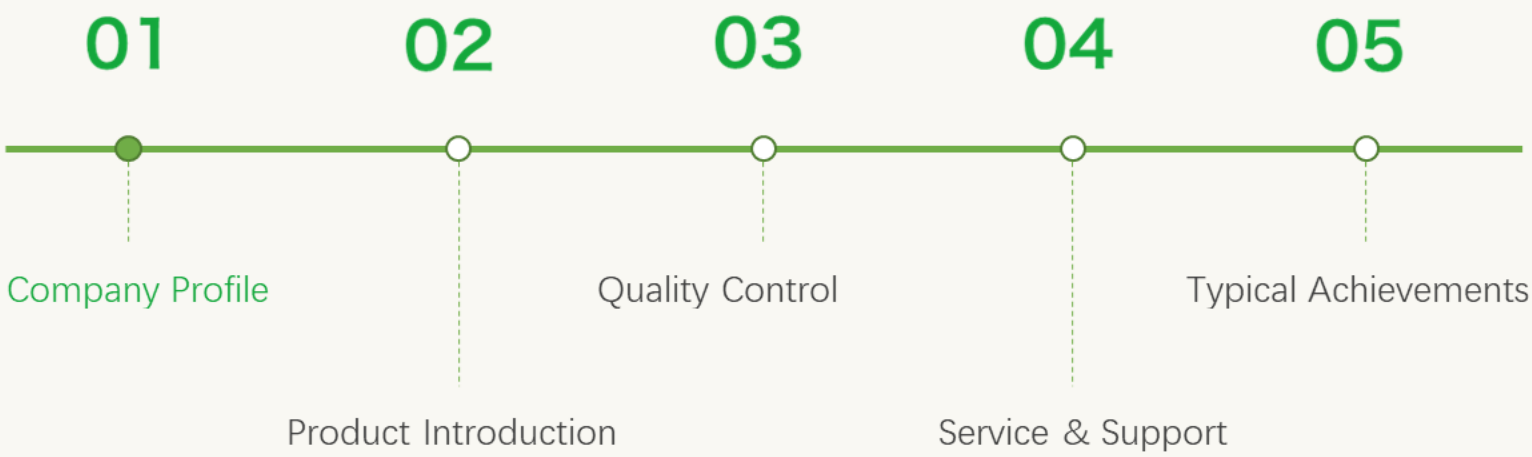
01
02
03
04
05
Company Profile
Product Introduction
Quality Control
Service & Support
Typical Achievements

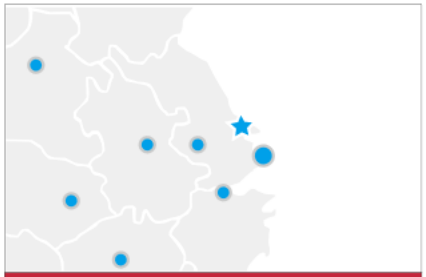

GTAKE

Think Without Boundary

Nantong, Jiangsu

Foundation & registration

Founded

Sept. 2009

Registered Capital

CNY 40 million

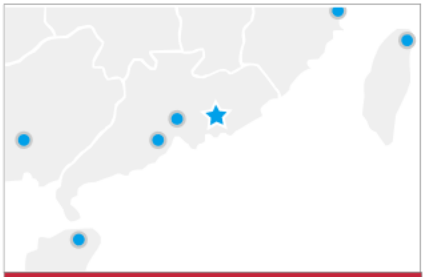

GTAKE

Think Without Boundary

Shenzhen, Guangdong

Headquarters

R&D and Manufacture center

Zhong-yun-tai Industrial Park,

Bao'an District, Shenzhen, China,

518108

Building Area : 8300m²

Employee: 340+

LV AC Drives

GK Series

ES Series

EV/HEV Motor Controllers

KTZ/KYS Series

FA Series

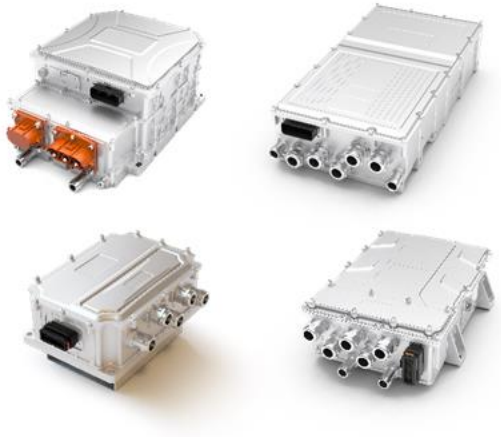

Wind Power Converters

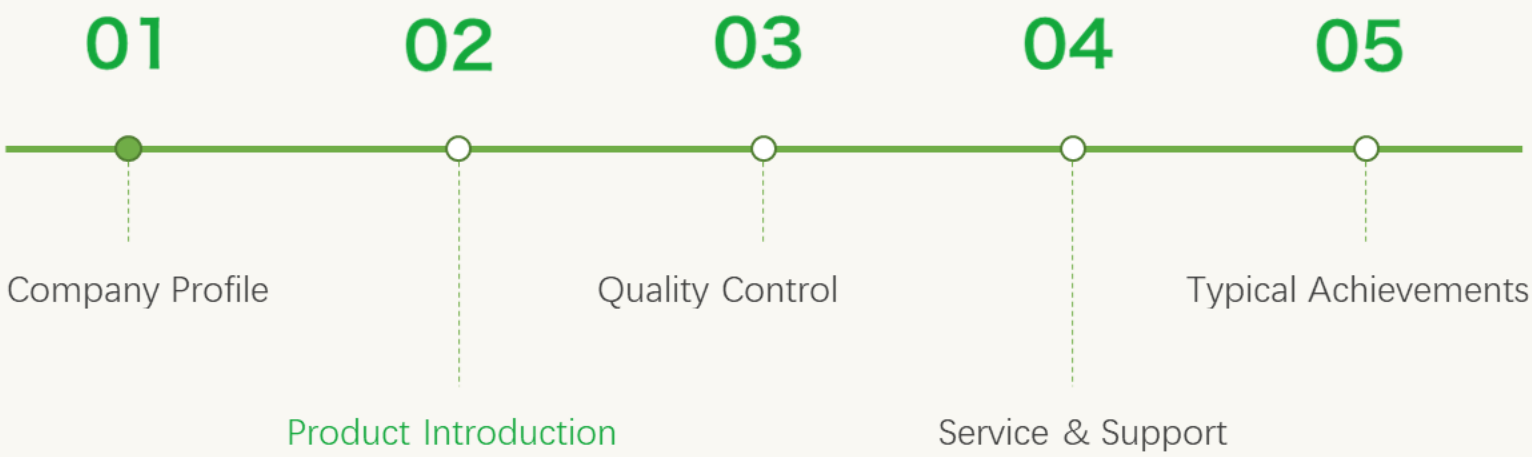
01
02
03
04
05
Company Profile
Product Introduction
Quality Control
Service & Support
Typical Achievements

ON-ROAD APPLICATIONS

Light EV

Passenger Car

Hybrid EV

E-Bus

Logistic Van

E-Motorcycle

OFF-ROAD APPLICATIONS *

Vessel

Crane

Digger & More···

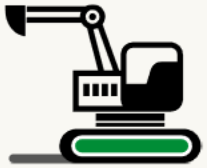

GTAKE EV/HEV Motor Controller

applied to many reputed vehicle manufacturers and powertrain enterprises

* Above are some of GTAKE cooperative enterprises, listed here with no precedence

High power density, high efficiency

Minimize the motor loss by unique control algorithm and PWM technology. The highest efficiency of the system is more than **95%**. The area of the efficiency over 85% exceeds **75%**.

** Wolong synchronous motor (peak 1500Nm, 80kW)*

System Efficiency	High efficiency area
95%	75%

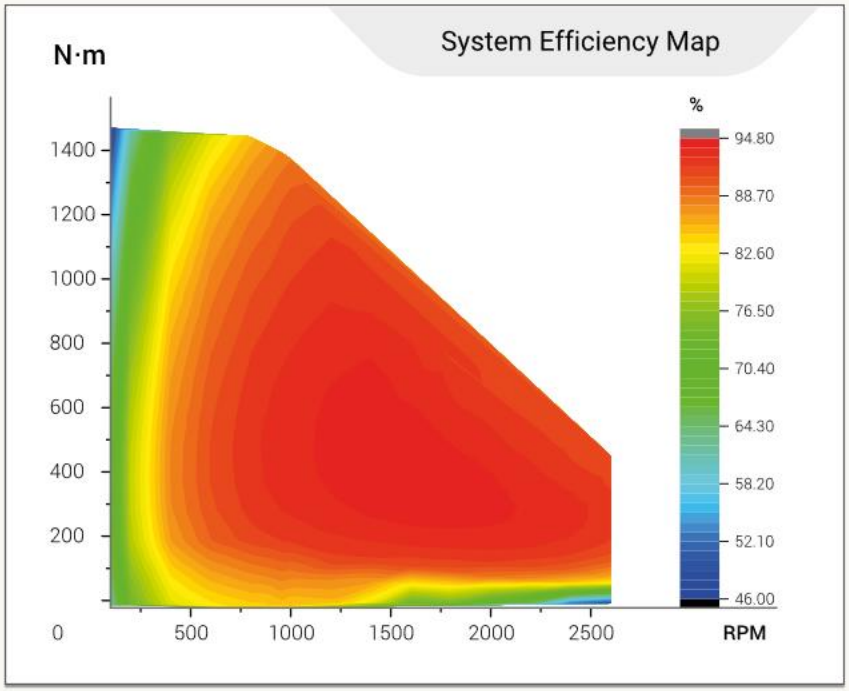

CUTTING-EDGE TECHNOLOGY

VS *REFERENCE SYSTEM

GTAKE self-developed algorithm enhances the output torque and speed stability at all required points, which extraordinarily extends the operation range and the vehicle efficiency effectively.

OPERATING VOLTAGE	540 VDC	540 VDC*
PEAK TORQUE	1470 N·m	1294 N·m *
CORNER SPEED	1378 RPM	1105 RPM *

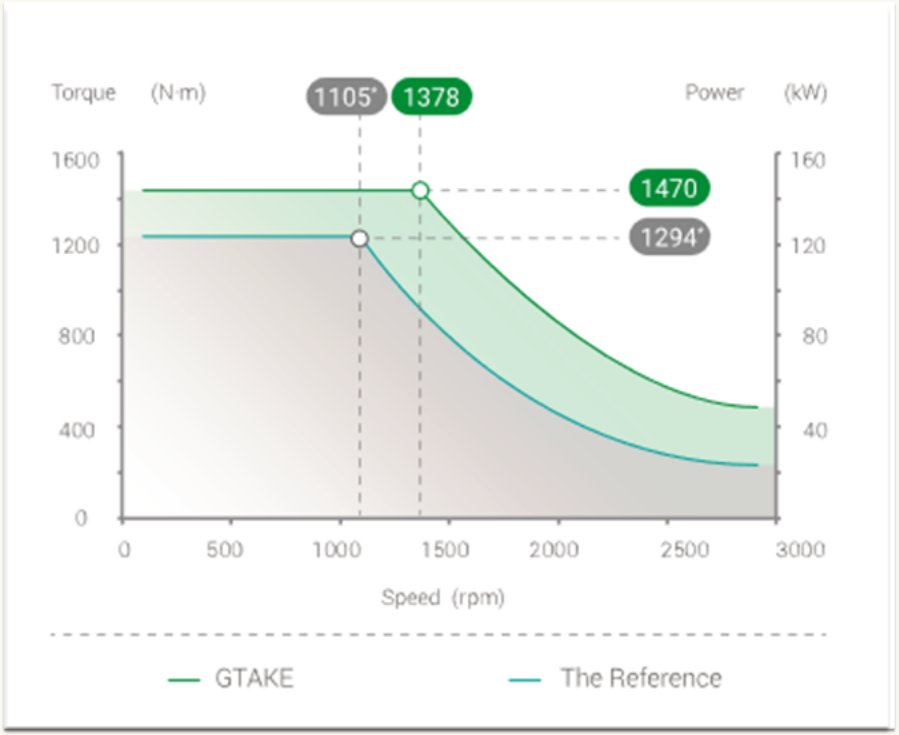

Meet the requirements of comfortability & stability

The vehicle can be well clamped on the slope automatically by a matching output torque, which is based on the position monitoring technology and switching tactics between torque control and speed control.

Less slope-slip distance and smooth quit of anti-slip function makes GTAKE a reputed brand in the EV industry.

1+N

MCU + DC/AC + DC/DC + AC/DC+ PDU+ Insulation detection

Frame	Main controller	Applicable to
G01	2Z45kW/4Z90kW	
G02	2Z75kW/2Z45kW/ 2Z80kW/2Z30kW	
G02A	2Z35kW/2Z25kW	
G03	4Z132kW/4Z90kW/ 4Z150kW	
G04	4Z160kW/4Z200kW	

Frame G02

Applicable to 8-meter-long buses, small trucks, light vans, economical MPVs

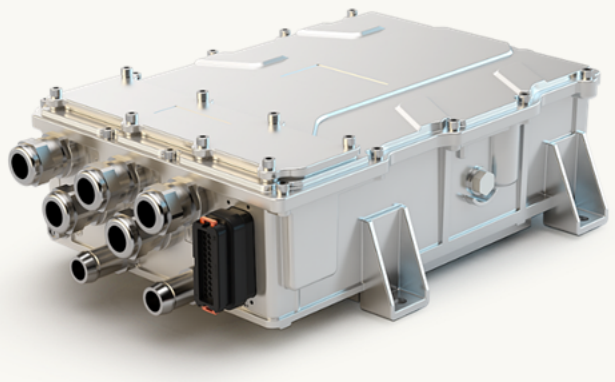

Model	KTZ54X41SAN**	KTZ54X32SAN**
MCU	4Z132kW	4Z90kW
Rated Power(kW)	132	90
Peak Power(kW)	198	135
Rated Output Current (A)	205	160
Peak Output Current (A)	410	320

9.8kg – 395×279×129.8mm

Water cooling **336（540）V** **IP67**

Frame G04

Applicable to 12-meter-long buses, middle-sized or heavy-duty trucks

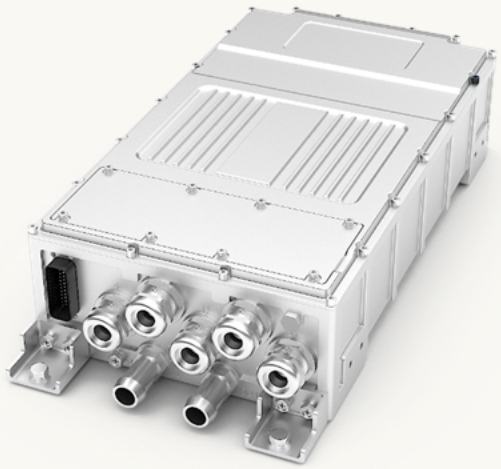

Model	KTZ54X57SH***	KTZ54X69SH***
MCU	4Z160kW	4Z200kW
Rated Power(kW)	160	200
Peak Power(kW)	240	300
Rated Output Current (A)	285	345
Peak Output Current (A)	570	690

22kg – 600×300×142.8mm

Water cooling

540 (336) V

IP67

Frame M10 (1+4)

Applicable to 8/10-meter-long buses and light trucks

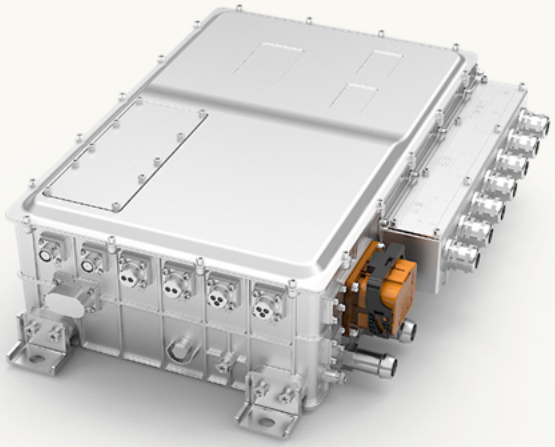

1 2

Model	KTZ54X41SU***	KTZ54X32SU***
MCU	4Z132kW	4Z90kW
Rated Power(kW)	132	90
Peak Power(kW)	198	135
Rated Output Current (A)	205	160
Peak Output Current (A)	410	320

1+4 – Traction motor drive+DC/AC×2+DC/DC+PDU

Water cooling

540 (336) V

IP67

Frame G05

Applicable to A0-level passenger cars

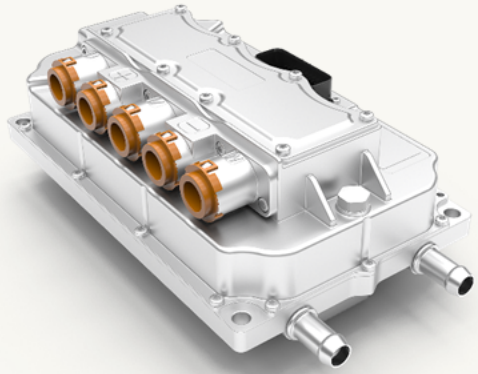

Model	KTZ34X30SDA**
MCU	2Z45kW
Rated Power(kW)	45
Peak Power(kW)	67.5
Rated Output Current (A)	150
Peak Output Current (A)	300

4.5kg – 280×176×120mm

Water cooling **336 V** **IP67**

Frame G05

Applicable to A0 level passenger cars

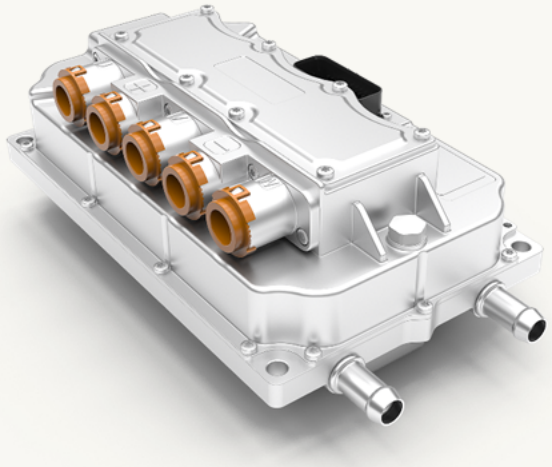

High power density: power density≥ 22.5kW/L, volume capacity<4.5L

No cable connection inside the controller

High protection grade, IP68 available

Vehicle dedicated IGBT and its operating temperature can reach up to 175°C

Frame G06

Applicable to A/B-level passenger cars

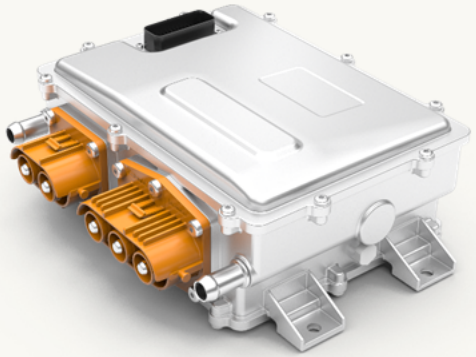

Model	KTZ34X45SCA**
MCU	2Z70kW*
Rated Power(kW)	70
Peak Power(kW)	100
Rated Output Current (A)	200
Peak Output Current (A)	450

9kg –289×188×121

Water cooling **336 V** **IP67**

Frame G06

Applicable to A0-level passenger cars

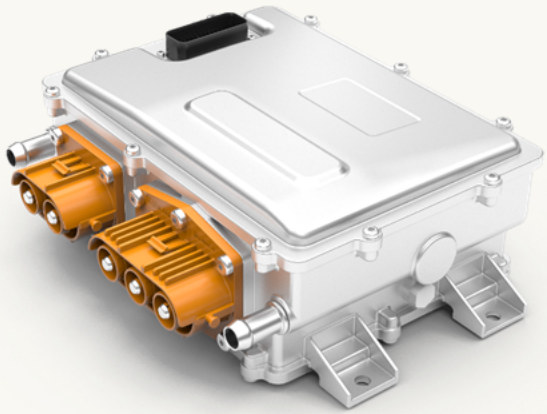

High power density

No cable connection inside the controller

High protection grade, IP68 available

The hardware design is according to ASIL-C and and its first safety mode is ASC (Active Short Circuit)

MCU adopts INFINEON vehicle dedicated platform

Vehicle dedicated IGBT

Power management and drive adopt vehicle dedicated IC

The software development is based on Autosar

MOSFET application: 2W

Vehicle type	E-bike	Scooter	E-Motocycle
Pic			
Max spd	⩽25Km/h	25-50Km/h	> 50Km/h
Weight	⩽55Kg	⩾55Kg	⩾55Kg
Bat vol	⩽48V	60-96	72-144
Mot Pwr	⩽400W	400W-4kW	> 4kW
Category	Non-motor	Motor	Motor
Mkt size	<1 mil	30 mil	<1 mil
License	x	√	√
Pedal	√	x	x
Plate	No	Blue	Yellow

Battery voltage (VDC)	Rated power (KW)	Product	Motor	Vehicle
48/60	2-3	D06	BLDC hub motor	
60/72	2-3.5 (3kW = 125cc)	D03	PMSM (high speed, mid drive)	
60/72/96	3.5-6	D03	PMSM (high speed, mid drive)	
72/96/144	7-15 (6kW = 250cc)	D04	PMSM (high speed, mid drive)	

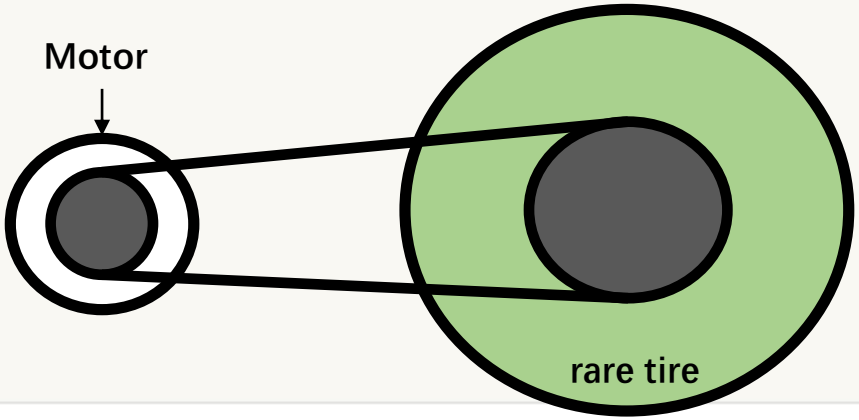

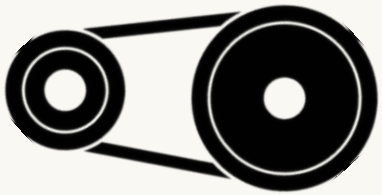
belt

chain

Vehicle test data (vs. competitor)

	Benchmark	Gtake	%
Date	2020 Feb		
Front tire pressure (psi)	22	22	-
Rare tire pressure (psi)	42	42	-
Battery voltage	83.5	83	-
Mileage (1 driver) (km)	91	100	10%
Mileage (1 pass) (km)	65	71	10%
Accel (1 driver) (m/s2)	1.38	1.38	-
Accel (1 pass) (m/s2)	0.5	1.11	120%
Max spd (1 drive) (kmph)	47	53	13%
Max spd (1 pass) (kmph)	44	54.5	24%
0-40kmph time (1)	8	8	-
0-40kmph time (2)	19	10	47%
10 dgr max spd (1) (kmph)	47.5	49	3%
10 dgr max spd (2) (kmph)	46	46	-
10 dgr 0-40 time (1)	10	8	20%
10 dgr 0-40 time (2)	18	10	44%

www.gtake.com.cn

Think Without Boundary

THANK YOU

Follow us on Wechat or visit official website to get more infomations & details.

GTAKE

Jie Dang
VP of internaltion business
j.dang@gtake.com.cn

AC Drive EV/HEV Motor Controller Wind-Power Converter Servo

Talk 2: PHM for EV battery

Panelist: Dr. Rui Zhao (National Research Council of Canada)

Research on Li-ion Battery Thermal Runaway

Rui Zhao

Research Council Officer

Energy, Mining and Environment Research Centre

Authors of TRIM: NRC : Dean MacNeil, Steven Recoskie, Oltion Kodra, Giulio Torlone, Joel Perron; Transport Canada : Kyle Hendershot

AGENDA

1. Li-ion Battery Background
2. Li-ion Battery Nail Penetration Coupling Model
3. Thermal Runaway Initiation Mechanism (TRIM)

1. Li-ion Battery Background

Applications

High energy density

Long lifespan

No memory effect

.
.
.

1. Li-ion Battery Background

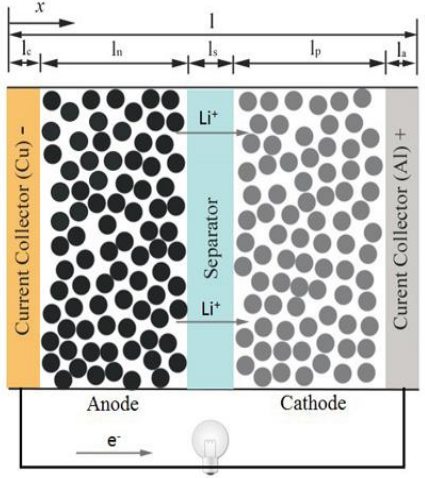

a

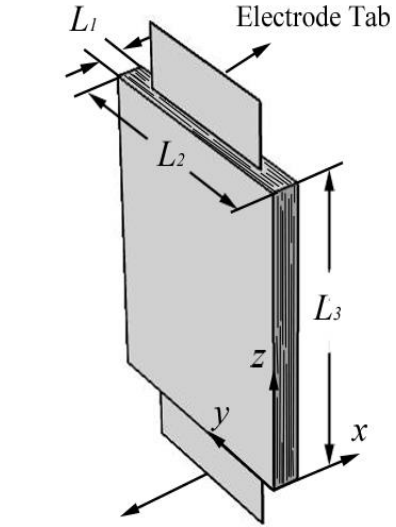

b

1. Li-ion Battery Background

Electrochemical Reaction

Exothermic Chemical Reaction

Short circuit

Overcharge

Overheat

1. Li-ion Battery Background

Some notable accidents induced by Li-ion batteries in recent years

Year	Accident	Causes
2019	Tesla Model 3 caught fire	Crash
2018	Porsche Panamera	Charging
2018	Kia Optima hybrid caught fire	Electrical issues
2017	Tesla Model S caught fire	Charging
2013	Tesla Model S caught fire	Vehicle hit metal debris
2013	Boeing 787 emergency landing	Battery overcharge
2012	BYD e6 caught fire	Crash
2011	Chevrolet Volt caught fire	Crash testing
2010	Acer recalled 2700 laptop batteries	Potential overheating and fire hazards

Thermal runaway (TR) research

2. Li-ion Battery Nail Penetration Coupling Model

0.65 Ah battery	no TR
1.2 Ah battery	TR
5 Ah thick electrode battery	
5 Ah thin electrode battery	TR with fire

2. Li-ion Battery Nail Penetration Coupling Model

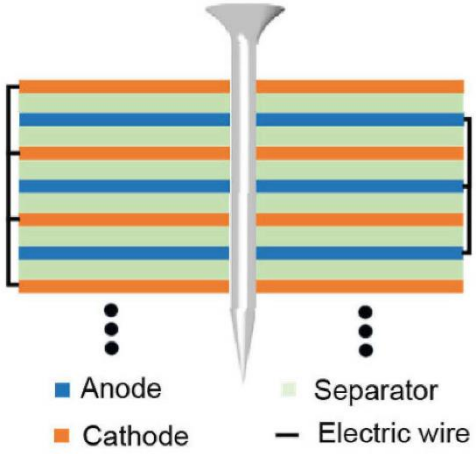

[1] Ref.: https://chemistry-europe.onlinelibrary.wiley.com/doi/abs/10.1002/batt.201900081

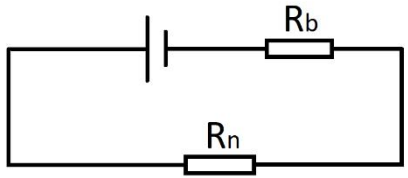

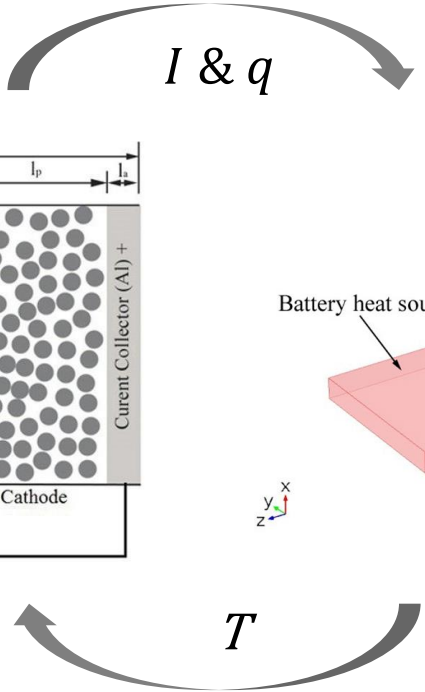

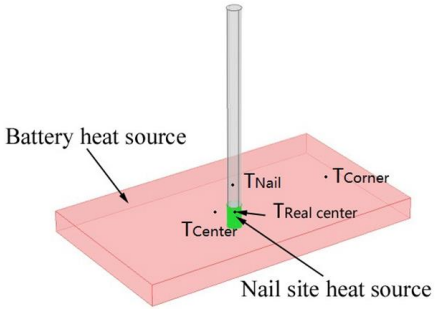

2. Li-ion Battery Nail Penetration Coupling Model

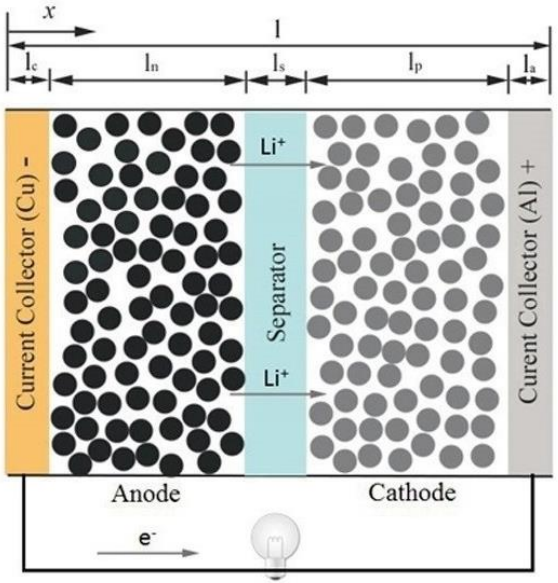

Equations used in the electrochemical model	
Material balance, electrolyte	$\varepsilon_e \frac{\partial c_e}{\partial t} = \frac{\partial}{\partial x}\left(D_e^{\text{eff}} \frac{\partial c_e}{\partial x}\right) + \frac{(1-t_+^0)}{F} j^{Li}$
Material balance, solid phase	$\frac{\partial c_s}{\partial t} = \frac{D_s}{r^2}\frac{\partial}{\partial r}\left(r^2 \frac{\partial c_s}{\partial r}\right)$
Charge balance, electrolyte	$\frac{\partial}{\partial x}\left(k^{\text{eff}} \frac{\partial \Phi_e}{\partial x}\right) + \frac{\partial}{\partial x}\left(k_D^{\text{eff}} \frac{\partial (ln\, c_e)}{\partial x}\right) = -j^{Li}$
Charge balance, solid phase	$\frac{\partial}{\partial x}\left(\sigma^{\text{eff}} \frac{\partial \Phi_s}{\partial x}\right) = j^{Li}$
Specific interfacial surface area	$a_s = \left(\frac{3}{R_s}\right)\varepsilon_s$
Reaction current density	$j^{Li} = a_s i_0 \left[exp\left(\frac{0.5F}{RT}\eta\right) - exp\left(-\frac{0.5F}{RT}\eta\right)\right]$
Overpotential	$\eta = \Phi_s - \Phi_e - U$

2. Li-ion Battery Nail Penetration Coupling Model

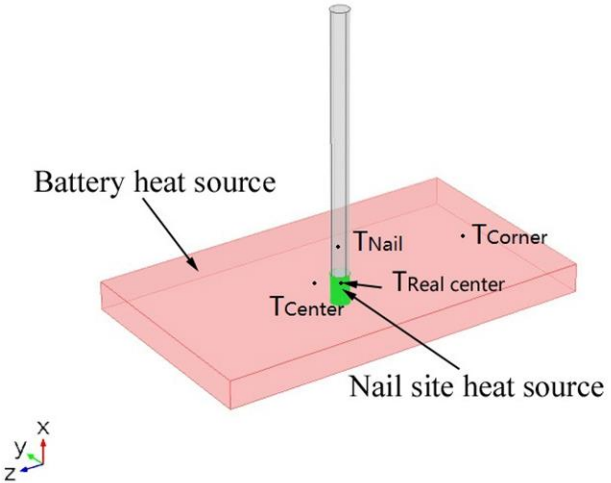

Equations used in the thermal model	
Energy conservation	$\rho C_p \frac{dT}{dt} = \nabla \cdot (k \nabla T) + q$
Reaction heat source	$q_r = \frac{\int_0^{l_n+l_s+l_p} j^{Li}(\Phi_s - \Phi_e - U)dx}{l}$
Ohmic heat source	$q_j = \frac{\int_0^{l_n+l_s+l_p} \left[\sigma^{\text{eff}} \left(\frac{\partial \Phi_s}{\partial x}\right)^2 + k^{\text{eff}} \left(\frac{\partial \Phi_e}{\partial x}\right)^2 + \frac{2k^{\text{eff}}RT}{F}(1-t_+^0)\frac{\partial(\ln c_e)}{\partial x}\frac{\partial \Phi_e}{\partial x}\right] dx}{l}$
Nail region heat source	$q_n = \frac{I_{dis}^2 \times R_n}{V}$

2. Li-ion Battery Nail Penetration Coupling Model

Contact Resistance

$$q_n = \frac{I_{dis}^2 \times R_n}{V}$$

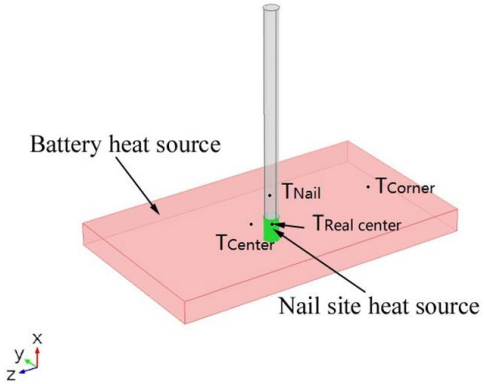

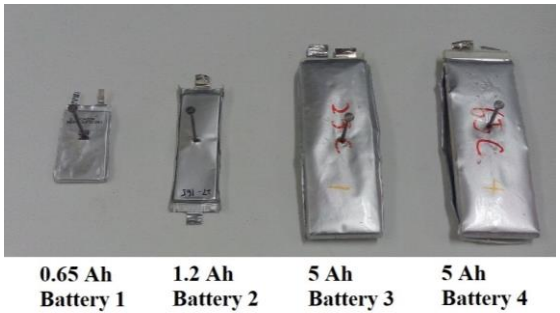

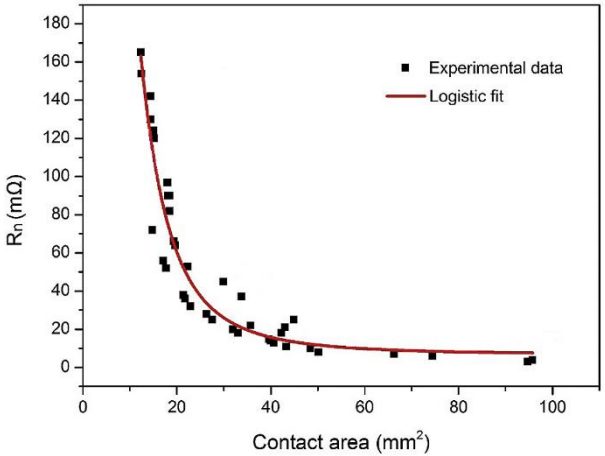

$$R_n = 6.7484 + \frac{545.877}{1 + \left(\frac{A}{8.77104}\right)^{2.69126}}$$

2. Li-ion Battery Nail Penetration Coupling Model

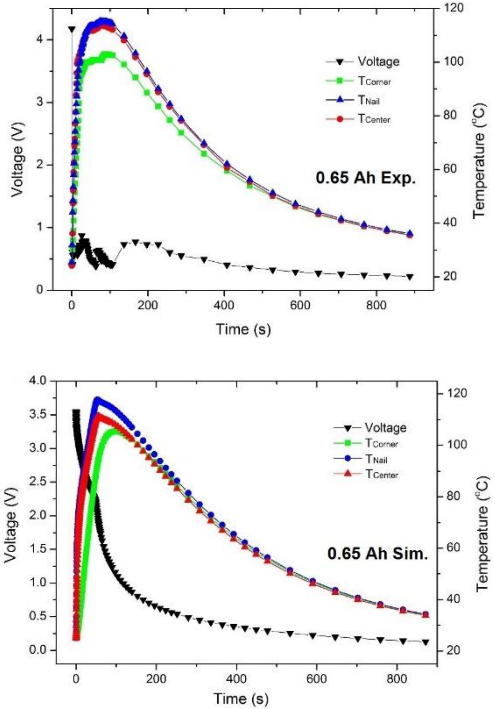

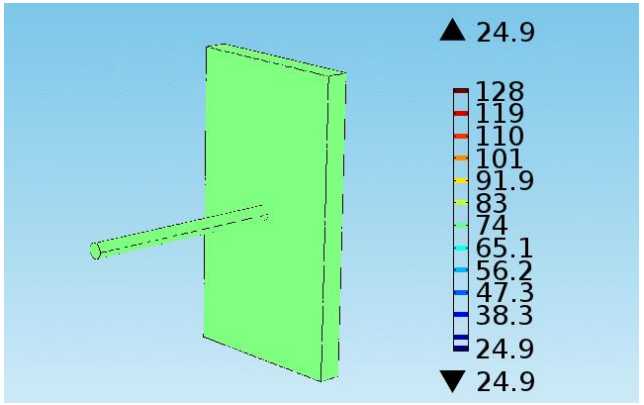

0.65 Ah battery temperature contour

2. Li-ion Battery Nail Penetration Coupling Model

1.2 Ah battery experiments

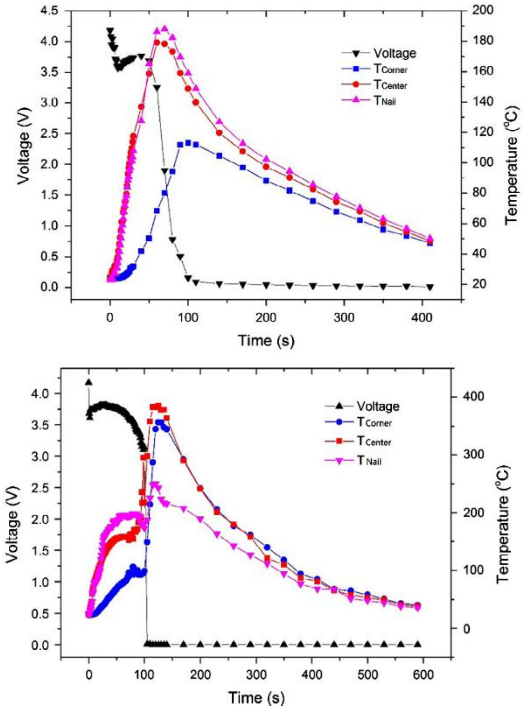

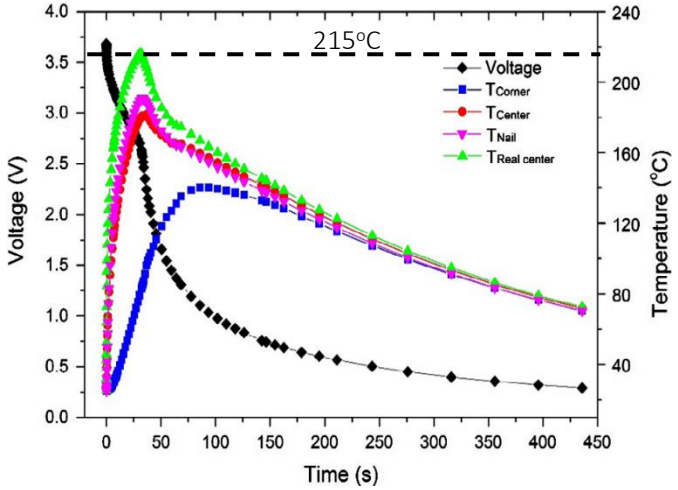

1.2 Ah battery simulation

Transition temperature of $LiCoO_2$ battery: **208 ±2°C** [2]

In simulation, the maximum temperature: **215 °C**

2. Li-ion Battery Nail Penetration Coupling Model

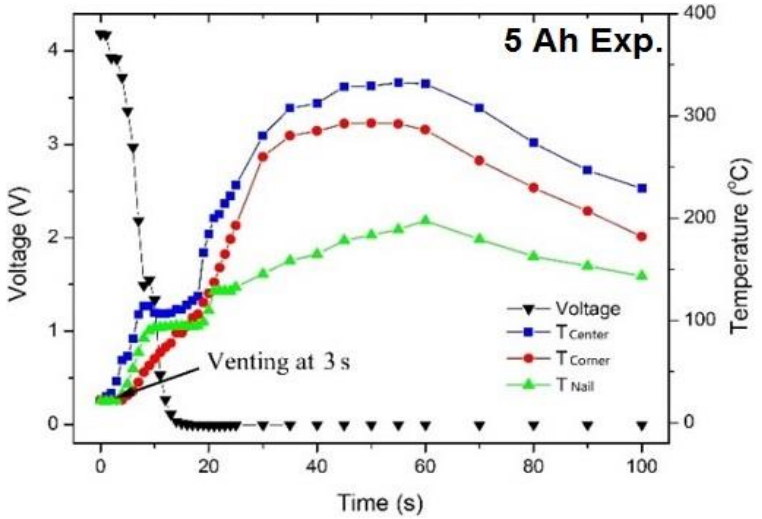

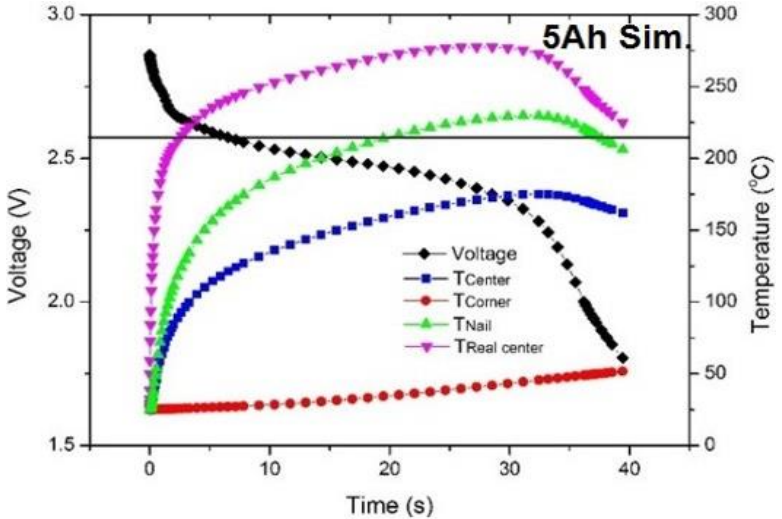

TR occurred at **3 s** in experiment and at **2.5 s** in simulation

3. Thermal Runaway Initiation Mechanism (TRIM)

In many situations, TR is not induced by crash, e.g., overcharge, overheat.

Reliable; Repeatable; Simple; No foreign holes; TR propagation research.

TRIM design
(WO2018132911A1)

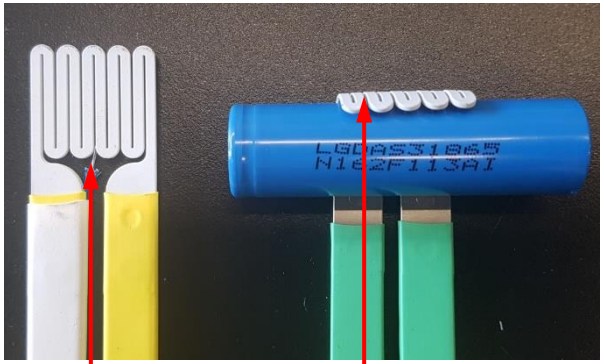

Formable to any cell (18650 shown)

Temperature feedback for optimized TR and element failure prevention

Key Parameters	Value
Thickness (mm)	1.0
Active Surface Area (cm^2)	5.6
Mass (g)	3.9
Peak Applied Power (W)	2000
Heat Flux (W/m^2)	> 1 x 10^6
Applied Energy compared to Type A cell capacity (%)	< 10

3. Thermal Runaway Initiation Mechanism (TRIM)

Concept of external heating

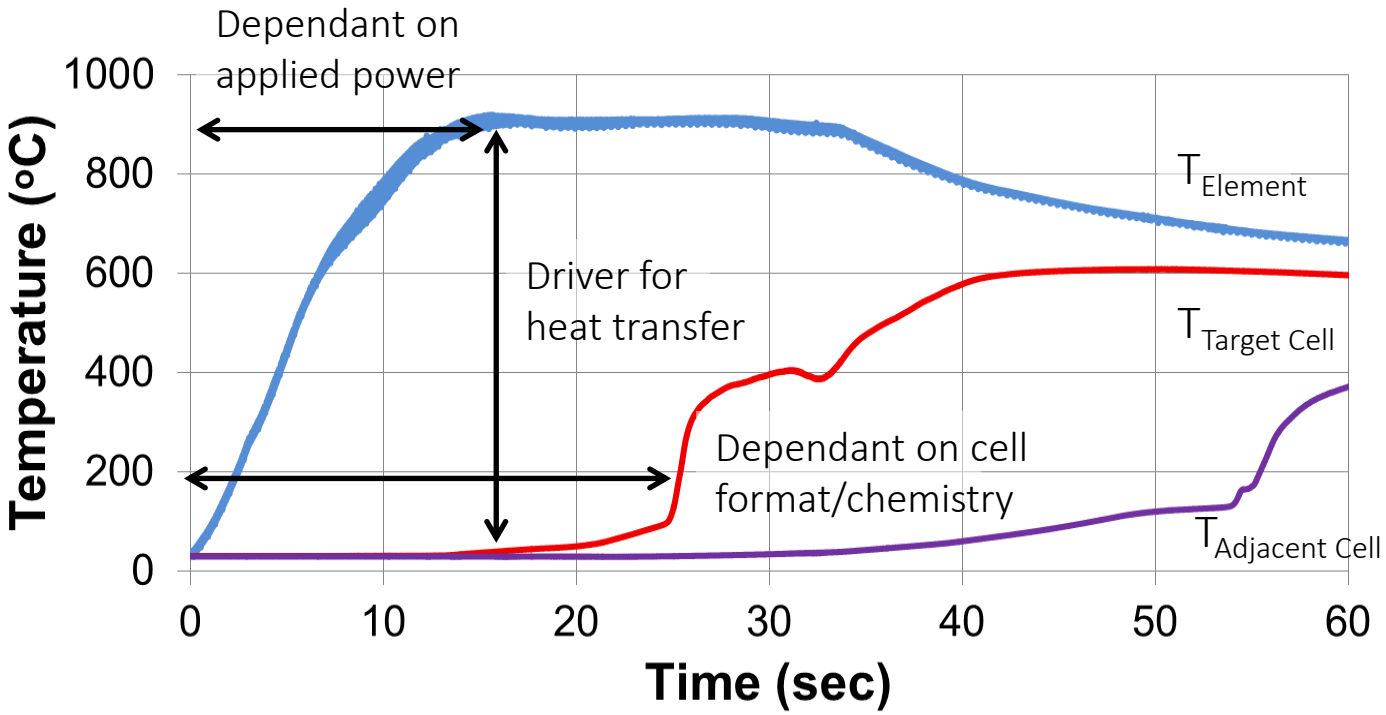

3. Thermal Runaway Initiation Mechanism (TRIM)

Test on Tesla Battery Pack

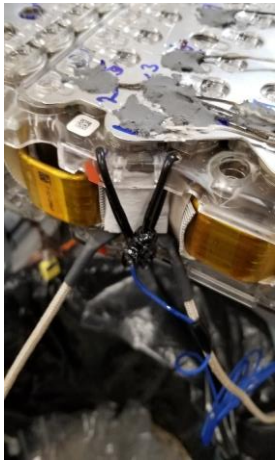

3. Thermal Runaway Initiation Mechanism (TRIM)

Test on Tesla Battery Pack

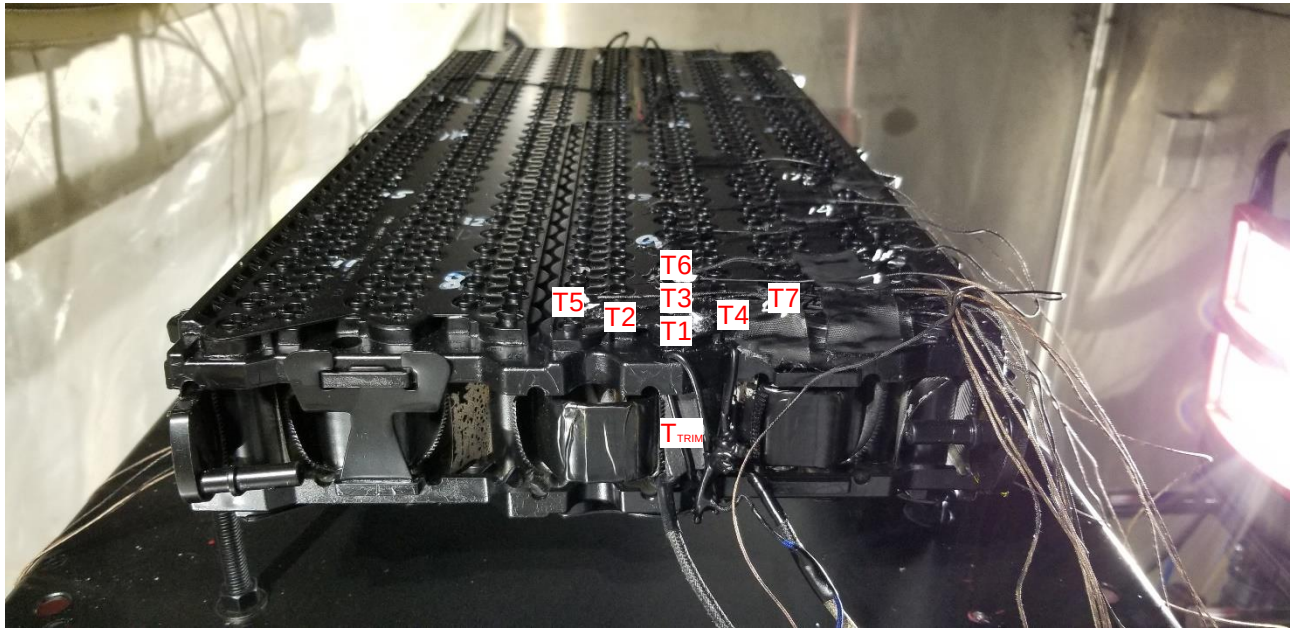

3. Thermal Runaway Initiation Mechanism (TRIM)

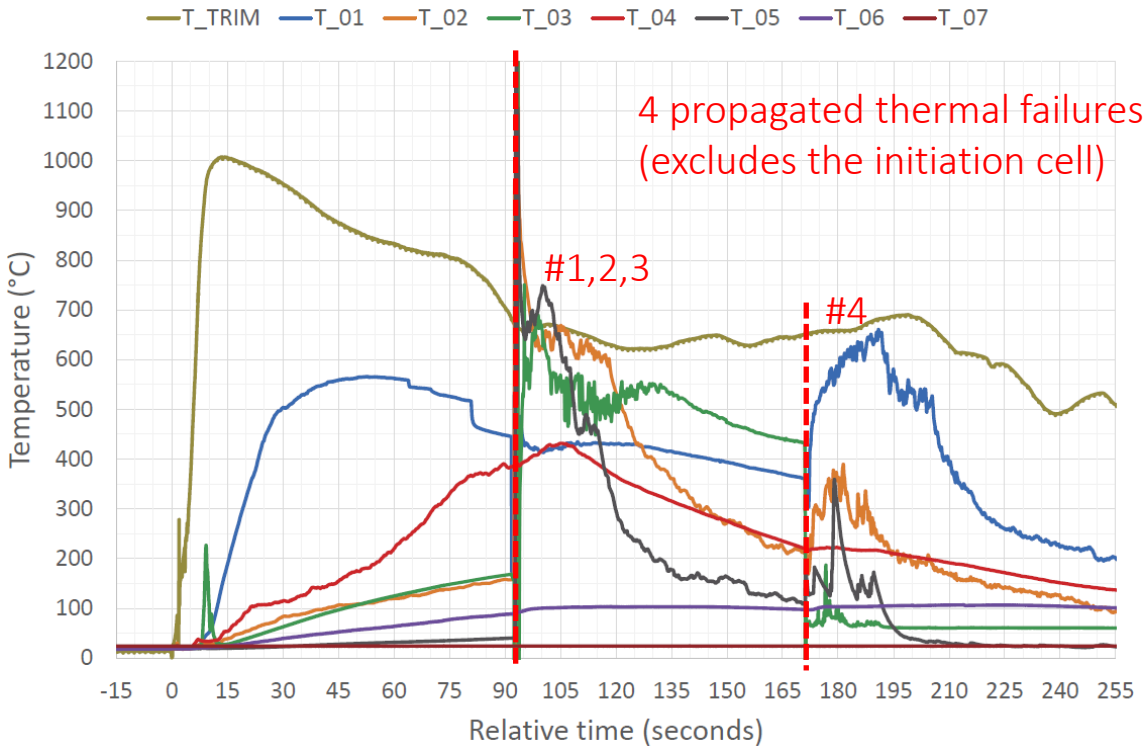

3. Thermal Runaway Initiation Mechanism (TRIM)

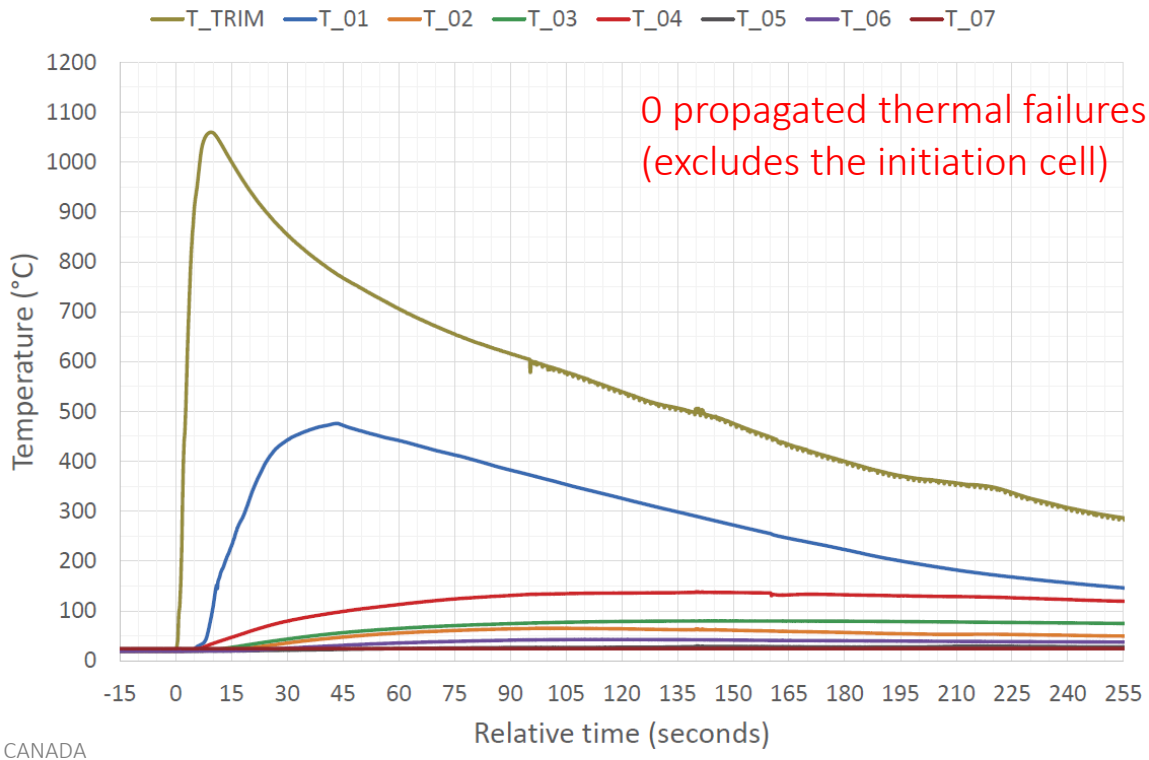

3. Thermal Runaway Initiation Mechanism (TRIM)

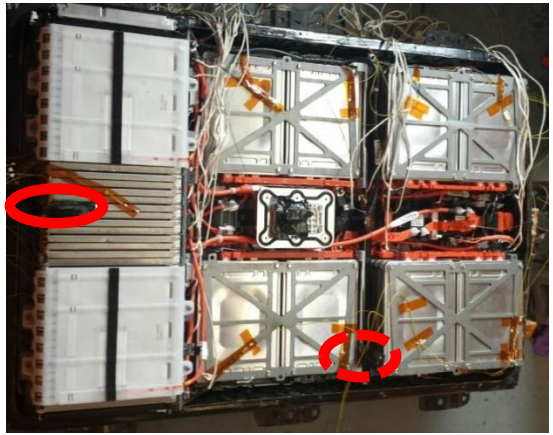

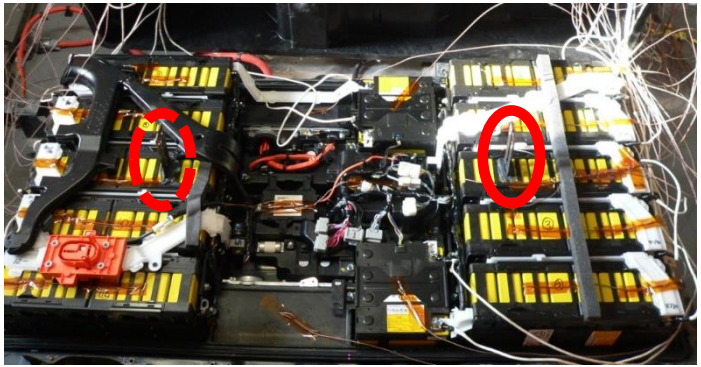

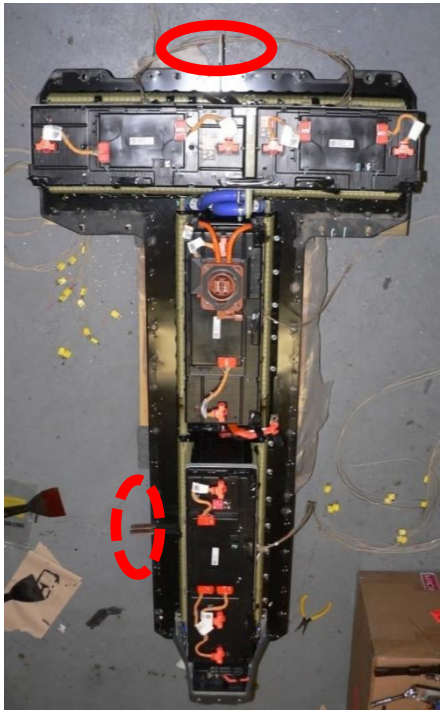

THANK YOU

Rui Zhao • Research Council Officer • Rui.Zhao@nrc-cnrc.gc.ca

For information about TRIM, please contact Steven Recoskie: Steven.Recoskie@nrc-cnrc.gc.ca

References

1. M. Chen et al. Batteries and Supercaps. 2019; 2: 874-881.
2. A.W. Golubkov et al. RSC Adv. 2014; 4: 3633–42.

Related Literature

1. R. Zhao, J. Liu, and J. Gu, Energy. Vol. 123, pp. 392-401, 2017.
2. R. Zhao, J. Liu, and J. Gu, Applied Energy. Vol. 173, pp. 29-39, 2016.
3. S. Recoskie, D. MacNeil, G. Torlone, O. Kodra, and J. Perron, Apparatus and method for initiating thermal runaway in a battery. WO 2018132911A1.

Talk 3: PHM for fuel cell systems

Panelist: Dr. Zhongliang Li (Aix-Marseille University, France)

PHM for fuel cell systems

Zhongliang LI

Laboratory of Information and System, Aix-Marseille University

Presented in PHMe 31/07/2019

Outline

- Why fuel cells (proton exchange membrane fuel cells)
- Why PHM for fuel cells
- Difficulties of PHM
- Open questions/research directions

Principle of proton exchange membrane fuel cell (PEMFC)

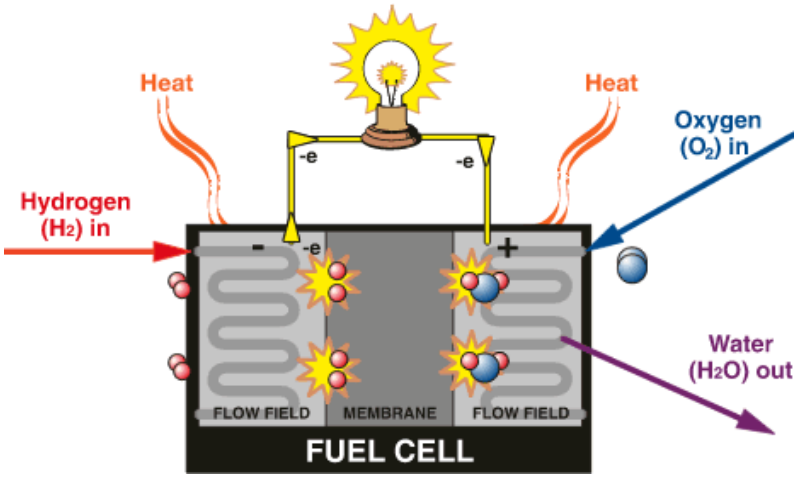

PEMFC single cell

anode: $H_2 \rightarrow 2H^+ + 2e^-$

cathode: $\frac{1}{2}O_2 + 2H^+ + 2e^- \rightarrow H_2O$

Fuel cell electric vehicle (FCEV)

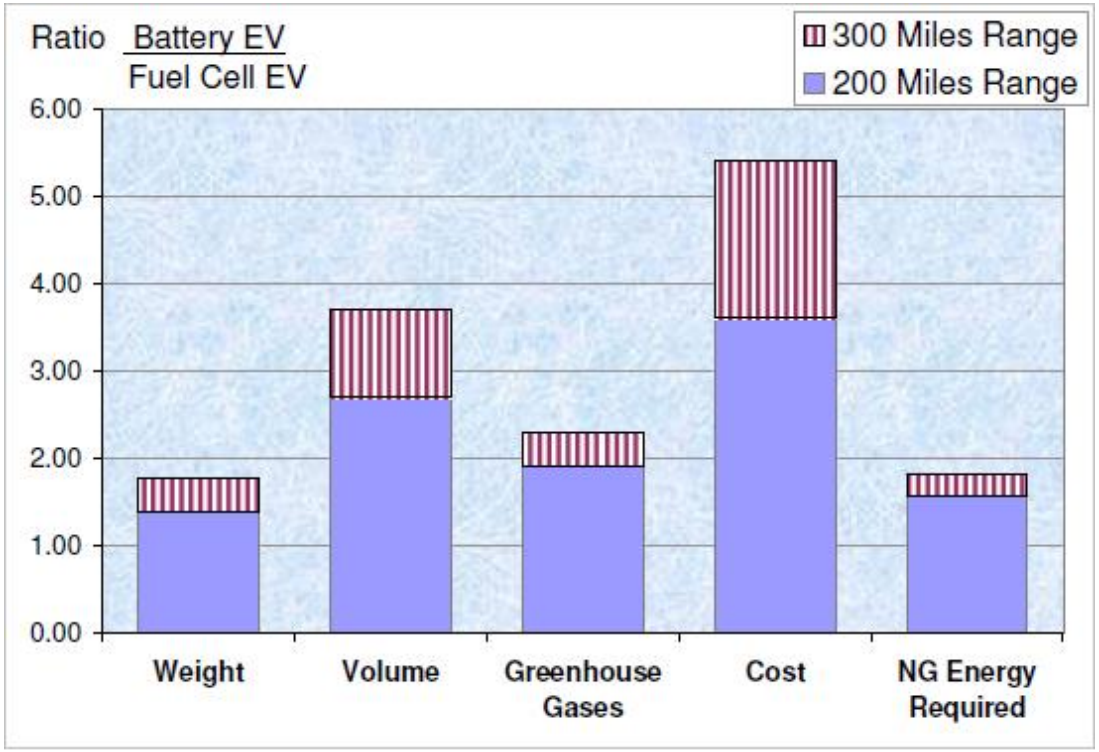

C.E. Thomas, International Journal of Hydrogen Energy, 2009

Toyota Mirai

Overview of Toyota Mirai	
Driving range	502 km
Fuel economy rating	3.6 L/100 km
Power	113 kW
Torque	335 Nm
Number of fuel cells	370
Power density	3.1 kW/L or or 2.0 kW/kg

Durability of fuel cells

Application		2020 DOE Durability Target[a]	Lab Status - Ave Hrs to 10% Voltage Degradation[b]
	Light Duty Automotive	5,000 Hours	3,700
	Public Transit	25,000 Hours	6,200
Stationary	1-10 kW 100 kW - 3 MW	0.3%/1,000 Hours 80,000 Hours	11,900
	Forklift	20,000 Hours - Target Under Review	13,500
	Backup	10,000 Hours - Target Under Review	2,600

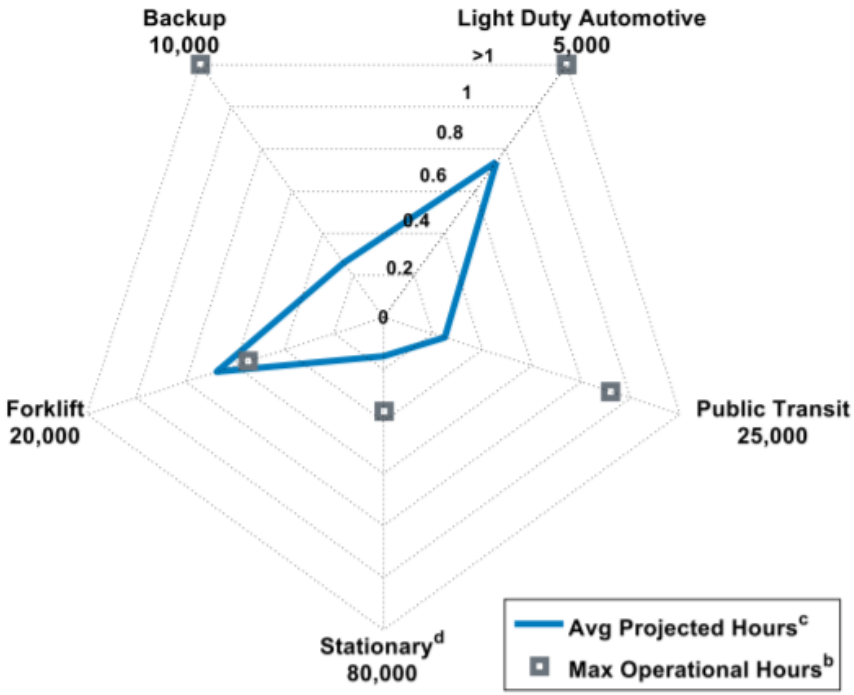

DOE 2017 Annual Merit Review . Department of Energy (DOE) US, June 8, 2017.

Difficulties of fuel cell PHM

Issue 1: Multiple subsystems, multiple physical processes

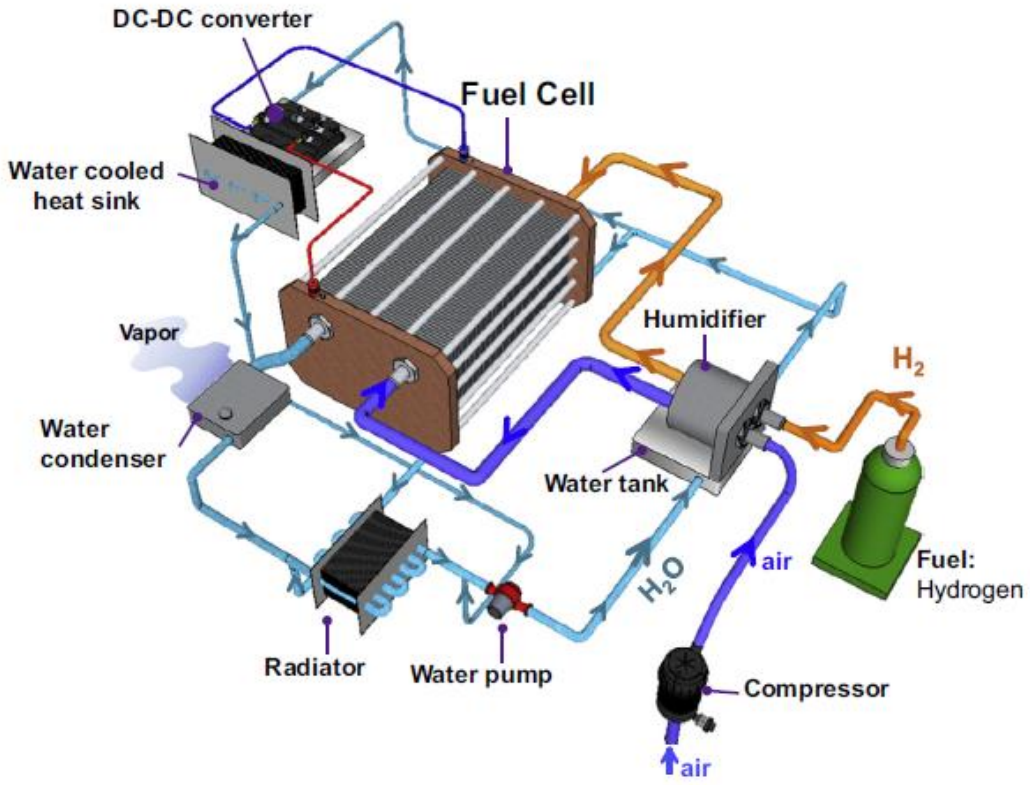

Difficulties of fuel cell PHM

Issue 2: Multi-time-scale and space-scale

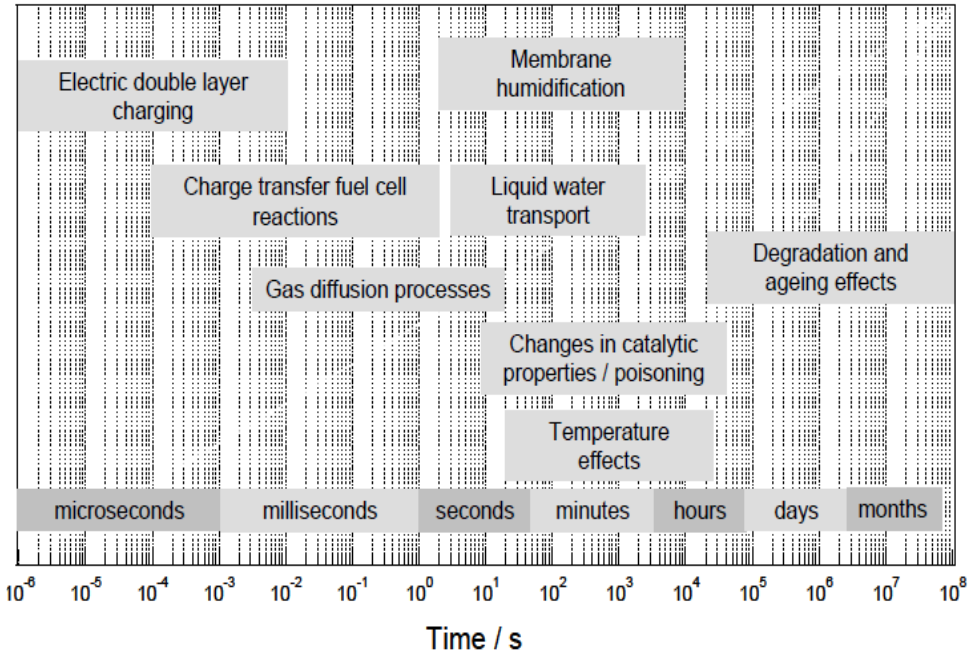

Hard to model…

Hard to explain…

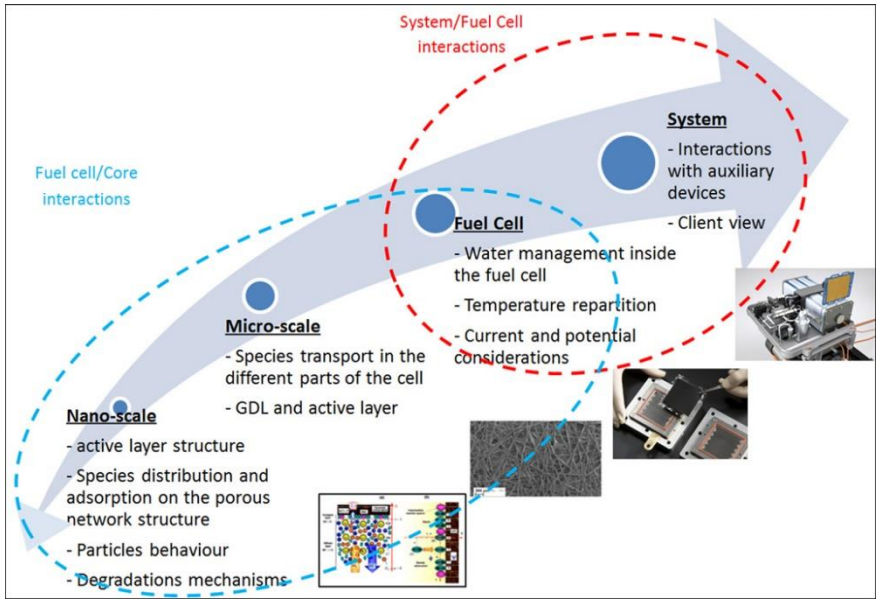

Difficulties of fuel cell PHM

Issue 3: High nonlinearity

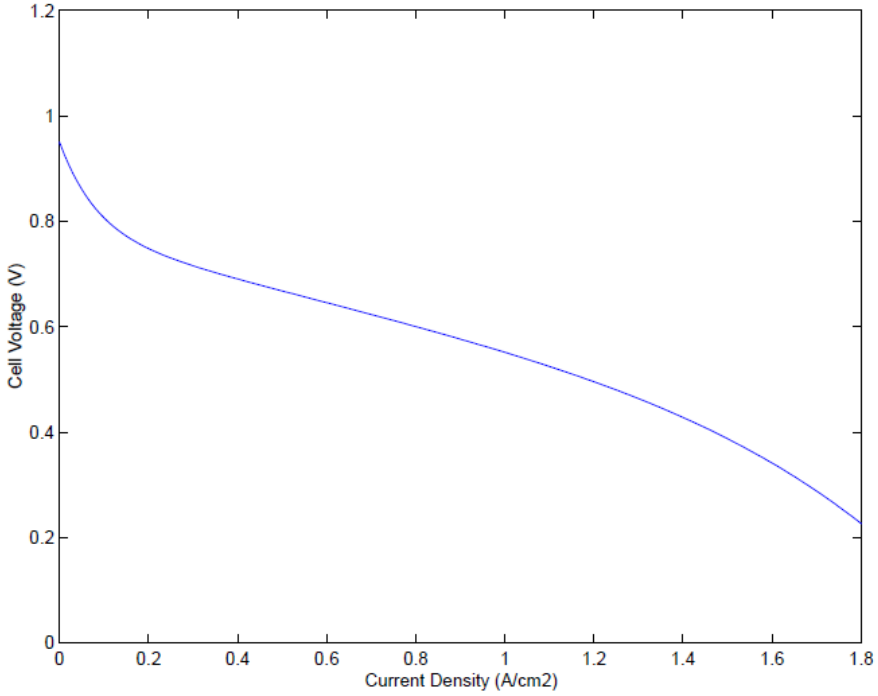

V-I characteristic

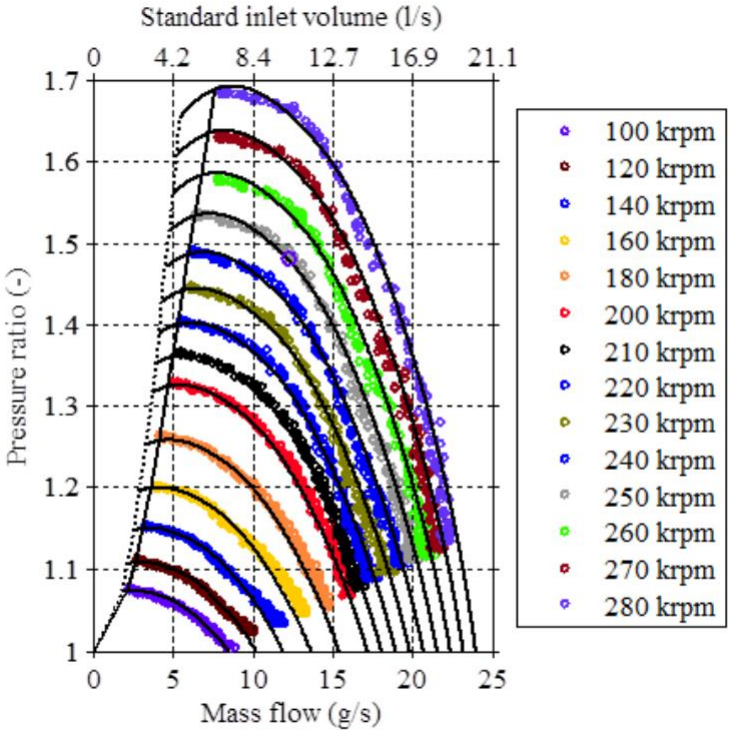

Pressure vs flow rate of compressor

Control issues of fuel cell systems

Issue 4: Multi-source system (system of systems)

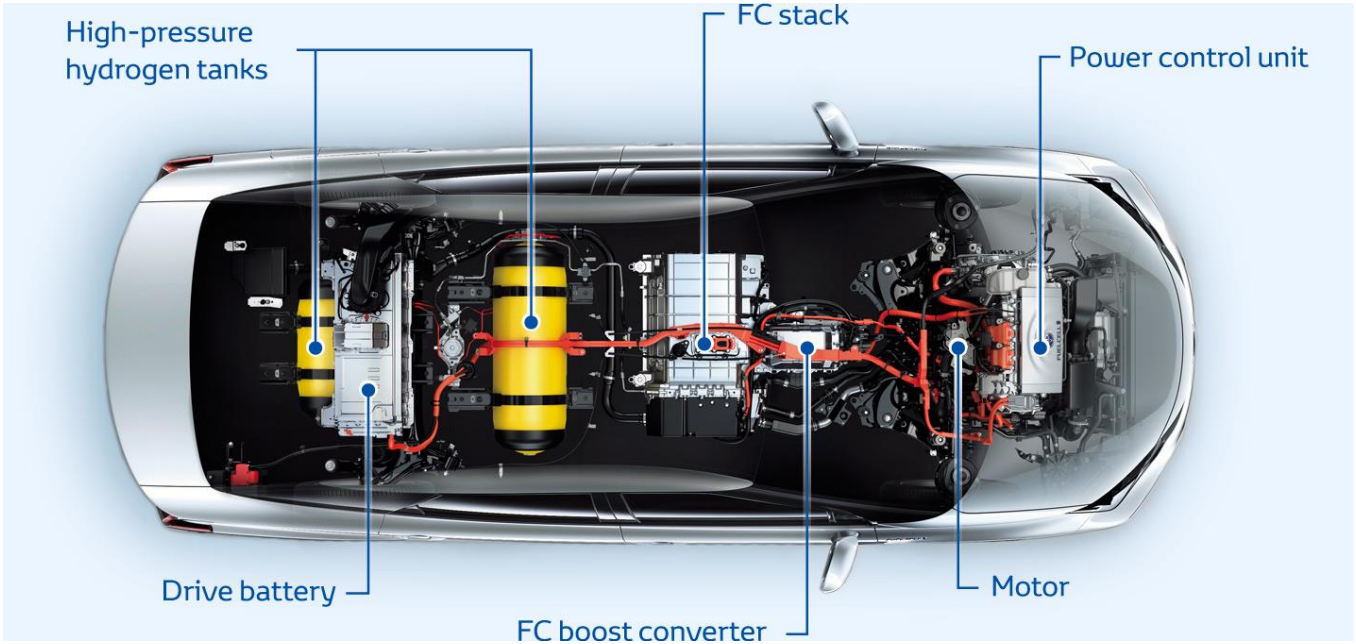

Open questions or ongoing works

- Topic 1: Knowledge of fuel cell degradation mechanism (ageing vs operating parameters).
- Topic 2: Ageing database (Accelerating degradation test).
- Topic 3: Develop in-situ degradation sensors/measurements.
- Topic 4: Improve the precision of multi-step ahead prediction and uncertainty evaluation.
- Topic 5: Improve the generalization ability of PHM methods.

More details:
Tutorial: Diagnosis, prognosis and fault tolerance control for fuel cell systems
October 18-21, IEEE IECON 2020

Thanks

Talk 4: MPC in EV applications

Panelist: Prof. Zhenbin Zhang, Mr. Yongdu Wang (Shandong University, China)

Predictive Control of 3L-NPC Converter Fed PMSM Drives for Electrical Car Applications

Presenter: Zhenbin Zhang

Yongdu Wang

Contact: zbz@sdu.edu.cn

School of Electrical Engineering
Shandong University
Jinan, China

Friday, 31/07/2020

Overview

1 Background

2 System description

3 Recent works

4 Experimental results

5 Summary

1. Background

Classification of Electric Vehicle

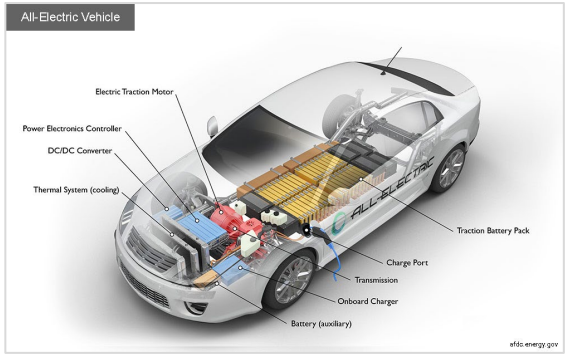

Battery Electric Vehicle (BEV)

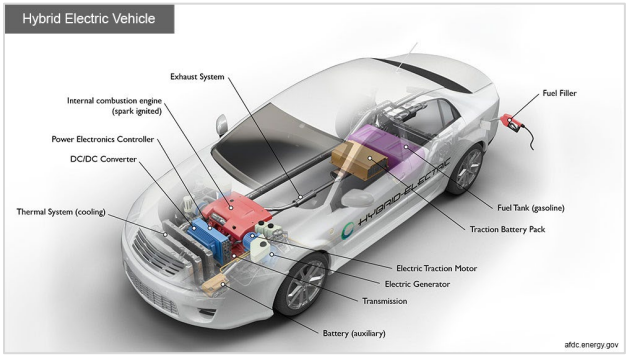

Hybrid Electric Vehicle (HEV)

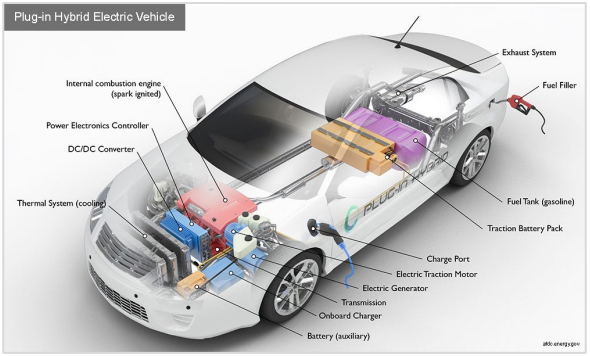

Plug-in Hybrid Electric Vehicle (PHEV)

Key technology

- **Vehicle control unit (VCU)**
- **Battery management system (BMS)**
- **Machine control unit (MCU)**

Reference: https://afdc.energy.gov/vehicles/how-do-all-electric-cars-work

1. Background

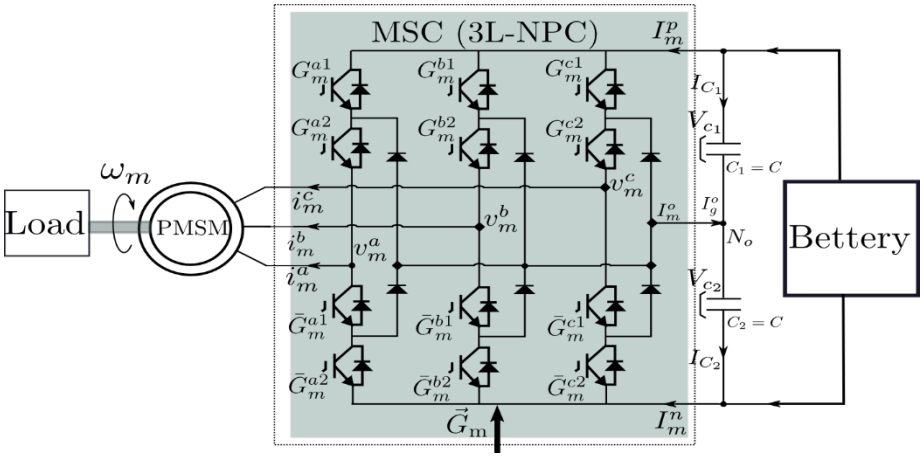

Fig.: Simplified electrical circuit of a 3L-NPC power converter fed PMSM drive.

Electrical drive system
- robustness
- reliability
- high energy density
- high efficiency

robustness → 3L-NPC
- handles high power ratings
- low (current or torque) THDs

high efficiency → PMSM
- higher energy density
- easy to control

1. Background

Vector Control (1st Gen)
- 1972
- Hasse (Germany)
- Blaschke (Germany)

Direct Control (2nd Gen)
- 1984
- Takahashi (Japan)
- Depenbrock (Germany)

Predictive Control
- J. Holtz (1983)
- R. Kennel (1984)
- J. Rodriguez (2004)

Vector Control

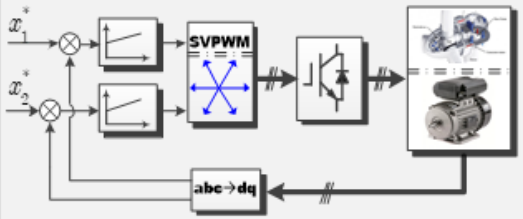

Single control objective

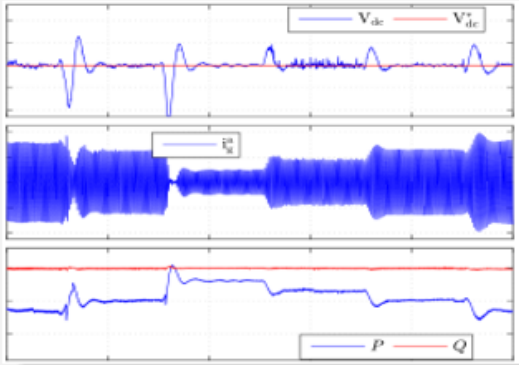

Direct Control

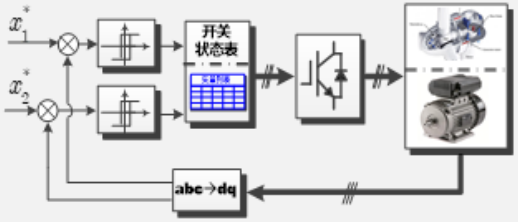

Local optimization

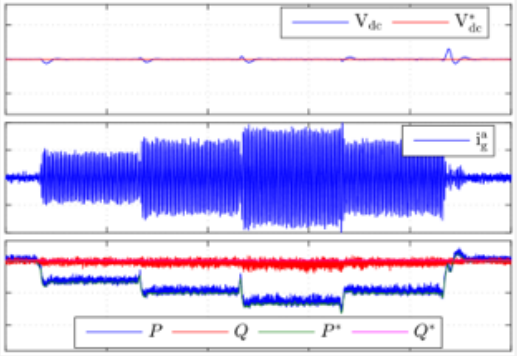

Limited control performance and flexibility

Predictive Control

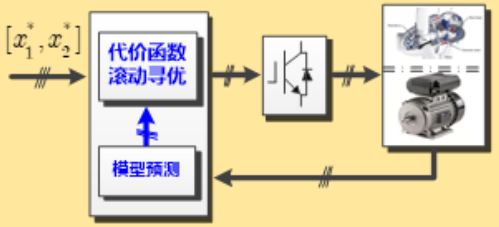

Multiple control objectives, global optimization, nonlinear constraints

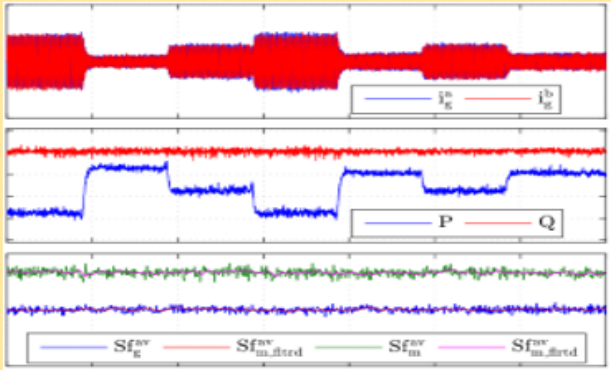

Very Powerful, Third Generation ①②③

① M. Kazmierkowski, IEEE Life Fellow, 2012; ② J. Rodriguez, IEEE Fellow, 2012; ③ R. Kennel, IET Fellow, 2001

1. Background

M. Kazmierkowski
IEEE Life Fellow

"Advance the performance of future energy processing and control systems"

Jose Rodriguez
IEEE Fellow

"Change dramatically how we control electrical energy using power electronics"

Ralph Kennel
IET Fellow, Director of EAL, TUM

"A simple and powerful method to control power converters and electrical drives"

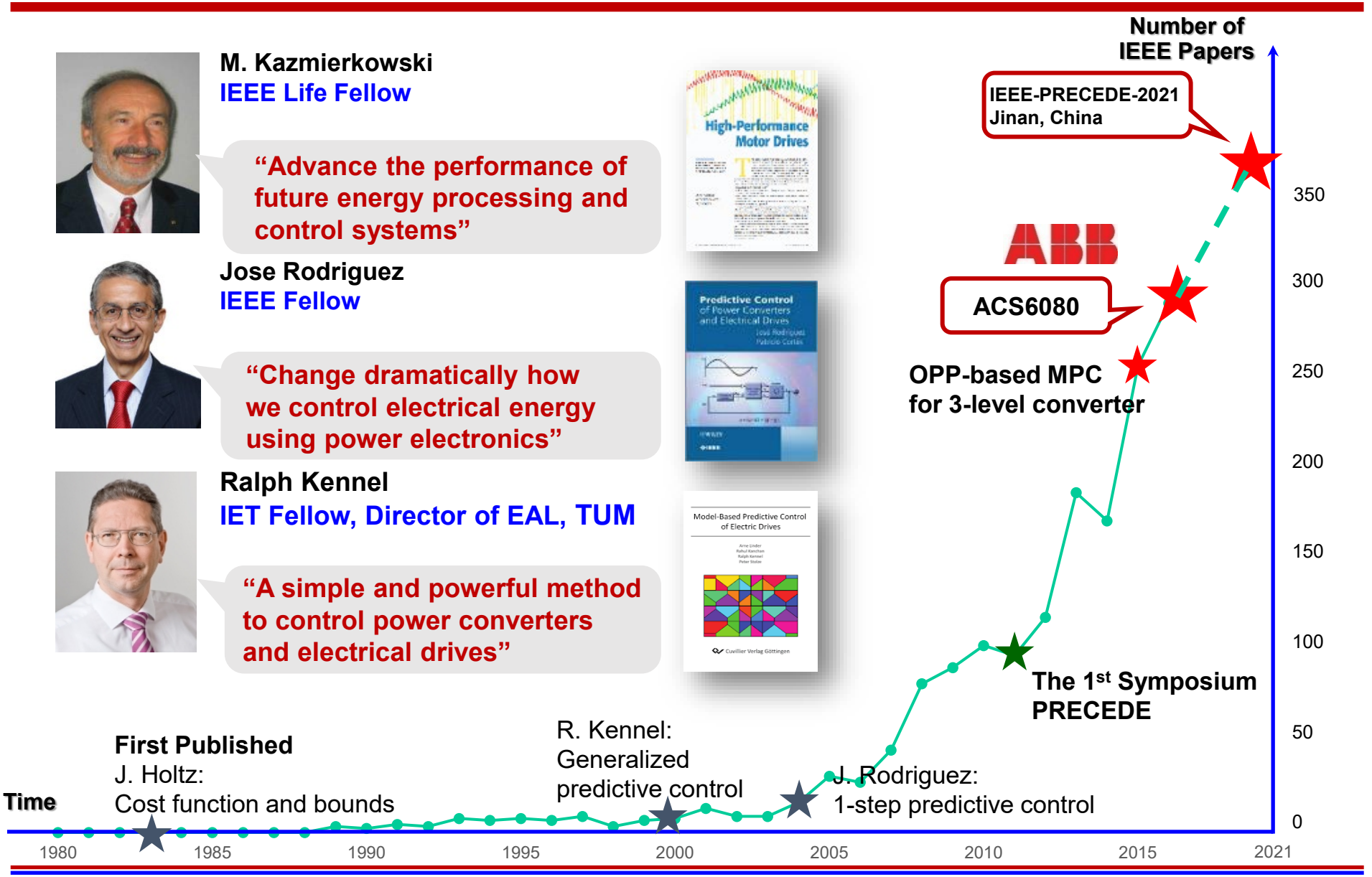

Control schemes

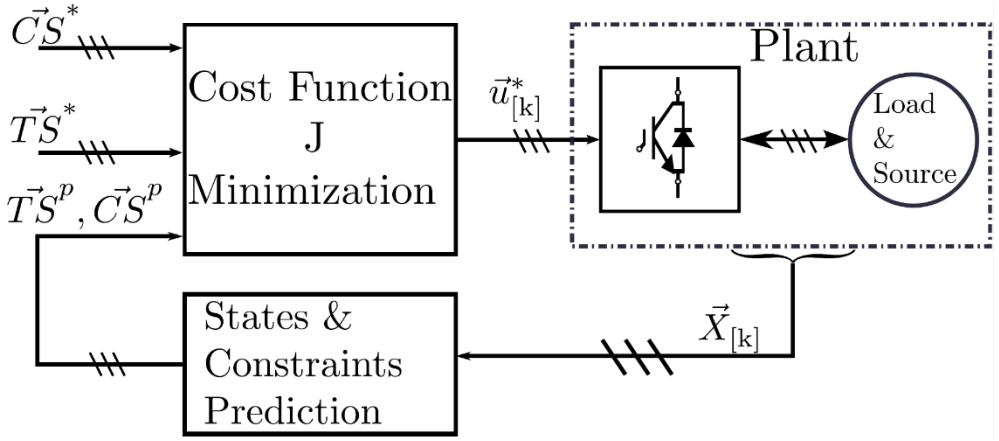

Fig.: Simplified structure of model predictive control for power electronics and drives.

Positive features:

- Straightforward design procedure
- Handling of complex & nonlinear dynamics
- Suitable for MIMO plants
- Achieving “customized” optimal control

Benefits:

- Improved plant performance
- Reduced engineering effort

1. Background

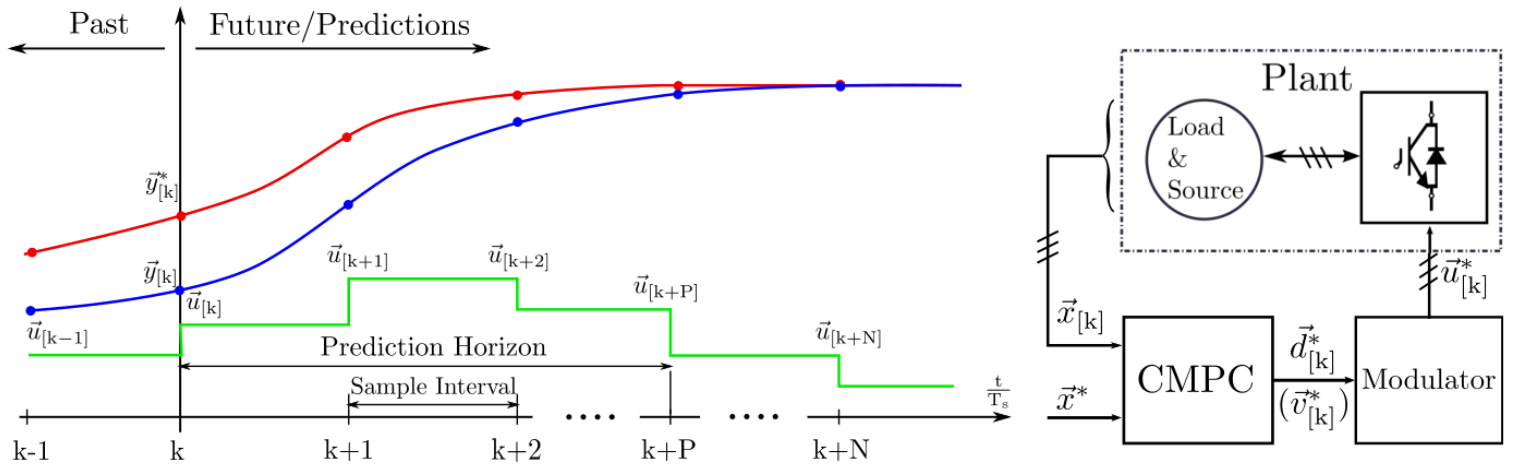

（a） General/continuous predictive control concept.(R.Kennel,et.al.,1983).

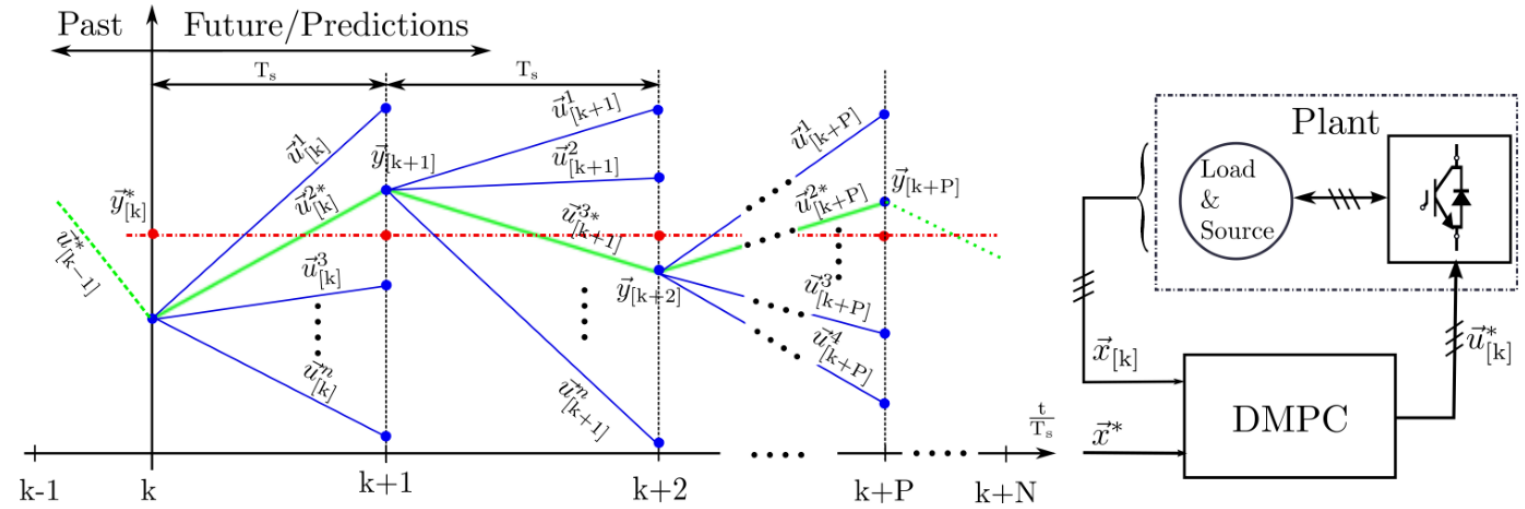

（b）Direct model predictive control concept.(J.Rodriguez,et.al.,2004).

Control schemes

But

- unmeasurable parameters (e.g., flux linkage)
- time-varying parameters (e.g., resistance and inductance)

Proposed method

A robust FCS-MPC control method with revised predictions

- Does not require extra fast sampling devices or parameter estimation techniques.
- The controller variable ripples are evidently reduced, at both the conditions with and without parameter variations.

2. System description

3L NPC back-to-back power converter

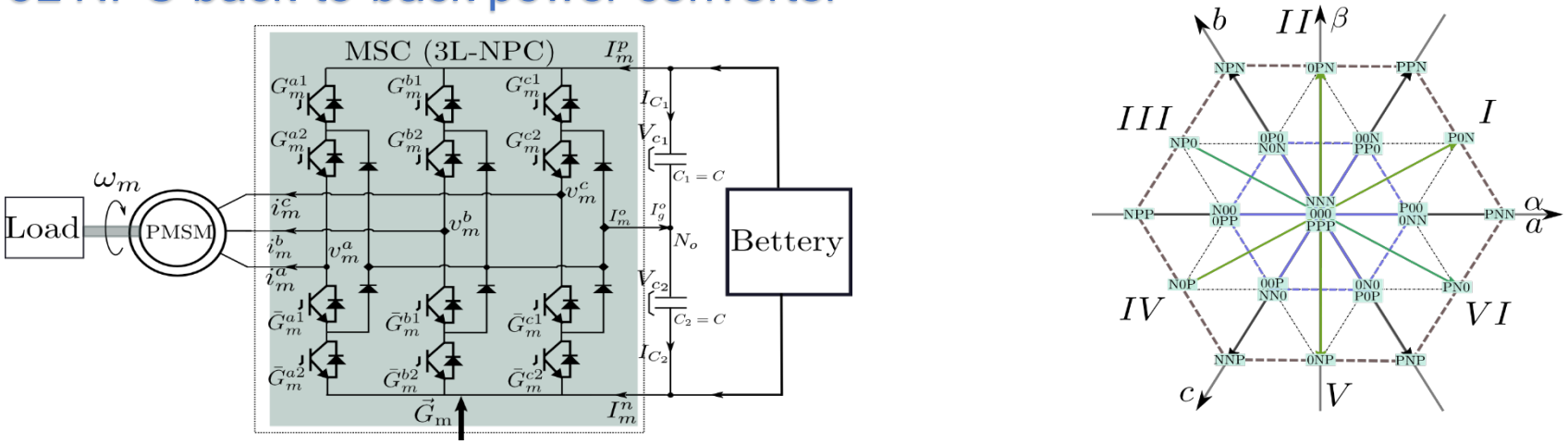

(a) (b)

Fig.: (a) Simplified electrical circuit of a 3L-NPC power converter fed PMSM drive used in an electric car and (b) switching vector planner.

PMSM

The discrete state space model

$$x_{\mathrm{m}}(k+1) = \mathbf{A}_{\mathrm{m}}(k) \cdot x_{\mathrm{m}}(k) + \mathbf{B}_{\mathrm{m}}(k) \cdot u_{\mathrm{m}}(k) + \mathbf{H}_{\mathrm{m}}(k) \quad \text{(Eq. 1)}$$

$$\mathbf{A}_{\mathrm{m}}(k) = \begin{bmatrix} 1 - \frac{T_{\mathrm{s}} R_{\mathrm{s}}}{L_{\mathrm{s}}} & T_{\mathrm{s}} \omega_{\mathrm{e}}(k) \\ -T_{\mathrm{s}} \omega_{\mathrm{e}}(k) & 1 - \frac{T_{\mathrm{s}} R_{\mathrm{s}}}{L_{\mathrm{s}}} \end{bmatrix}, \quad \mathbf{B}_{\mathrm{m}} = \begin{bmatrix} \frac{T_{\mathrm{s}}}{L_{\mathrm{s}}} & 0 \\ 0 & \frac{T_{\mathrm{s}}}{L_{\mathrm{s}}} \end{bmatrix}, \quad \mathbf{H}_{\mathrm{m}}(k) = \left(0, -\frac{T_{\mathrm{s}} \psi_{\mathrm{pm}}}{L_{\mathrm{s}}} \omega_{\mathrm{e}}(k)\right)^{\top}$$

3. Recent works

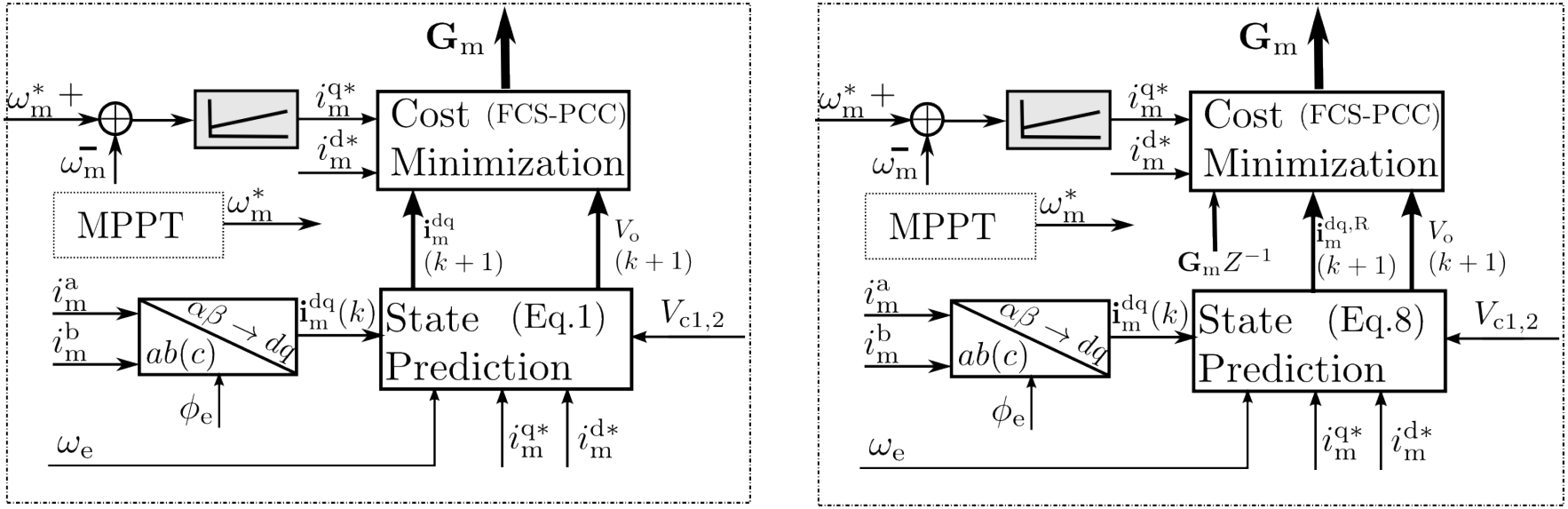

Fig.: Structure of (a) the classical and (b) the proposed FCS-MPC.

Model predictive control

(co_1) Torque/current control: Low torque ripples and low THDs must be guaranteed.

(co_2) Voltage balancing: The controller needs to assure voltage balancing in upper and lower DC-link capacitors.

(co_3) Switching frequency regulation.

Paper: "Robust Predictive Control of 3L-NPC Converter Fed PMSM Drives for Electrical Car Applications"

3. Recent works

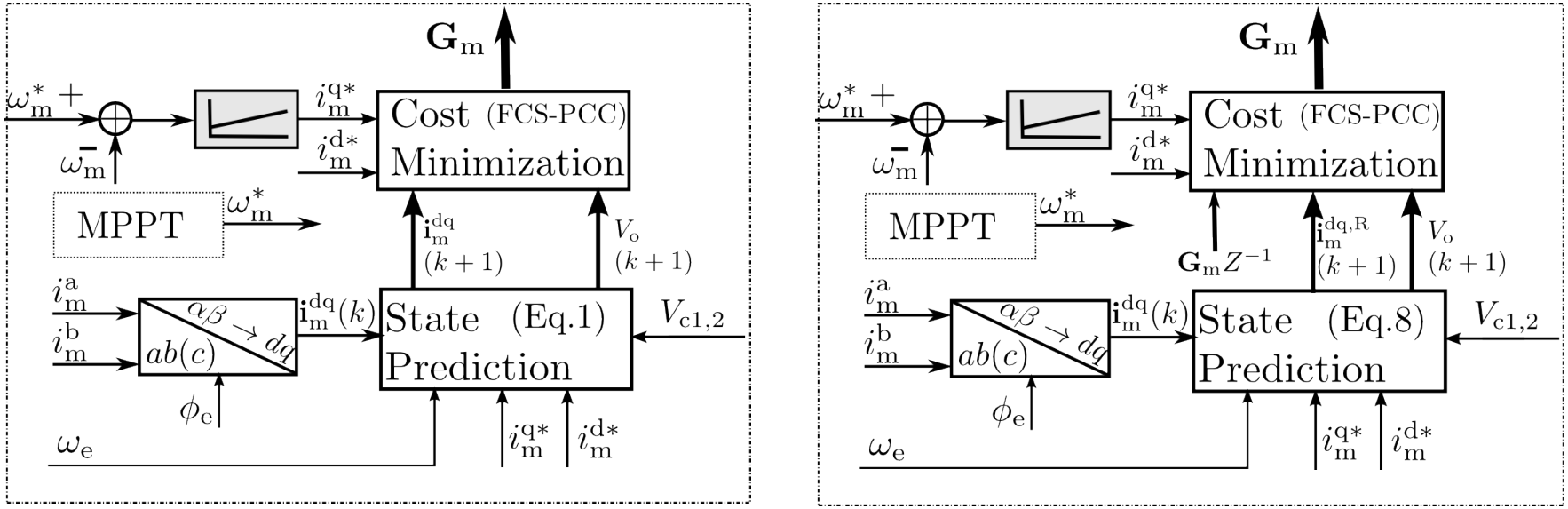

(a) (b)

Fig.: Structure of (a) the classical and (b) the proposed FCS-MPC.

Model predictive control

$$J_\mathrm{m}(\boldsymbol{u}_\mathrm{m}) = \boldsymbol{\Gamma}_\mathrm{m}||\boldsymbol{x}_\mathrm{m}^* - \boldsymbol{x}_\mathrm{m}(k+1)||^2 + \gamma_\mathrm{m}^{\mathrm{sf}}\Delta_{\boldsymbol{u}_\mathrm{m}} + \gamma_\mathrm{m}^{V_o}(V_o^* - V_o\,(k+1))^2 \qquad \text{(Eq. 2)}$$

where $\boldsymbol{\Gamma}_\mathrm{m} = \begin{bmatrix} \gamma_{i_\mathrm{m}}^{\mathrm{d}} & 0 \\ 0 & \gamma_{i_\mathrm{m}}^{\mathrm{q}} \end{bmatrix}$, $\gamma_{i_\mathrm{m}}^{\mathrm{q}}[1]$, $\gamma_{i_\mathrm{m}}^{\mathrm{d}}[1]$, $\gamma_\mathrm{m}^{V_o}[1]$ and $\gamma_\mathrm{m}^{\mathrm{sf}}[1]$ are weighting factors.

$$\Delta_{\boldsymbol{u}_\mathrm{m}} = \sum_{i=a,b,c} \left(|u_\mathrm{m}^{\mathrm{i}}(k+1) - u_\mathrm{m}^{\mathrm{i}}(k)|\right) \qquad \text{(Eq. 3)}$$

3. Recent works

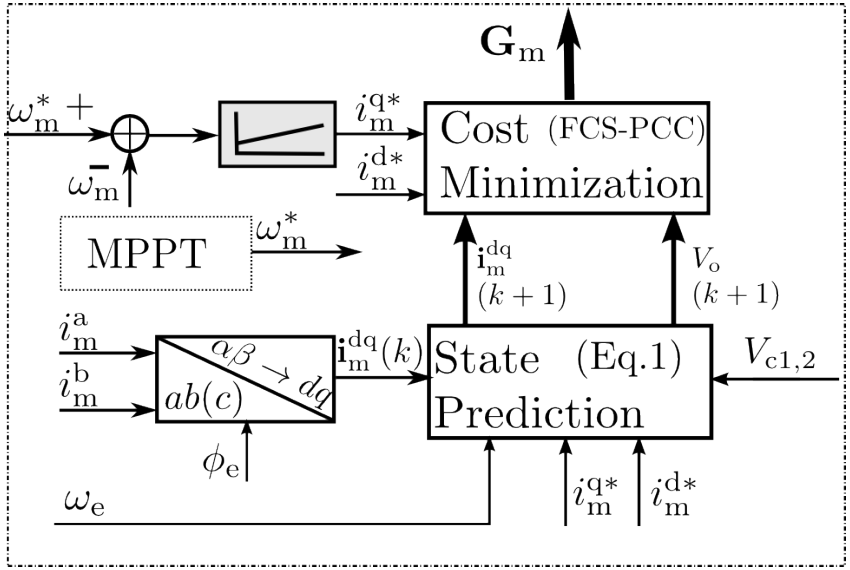

(a)

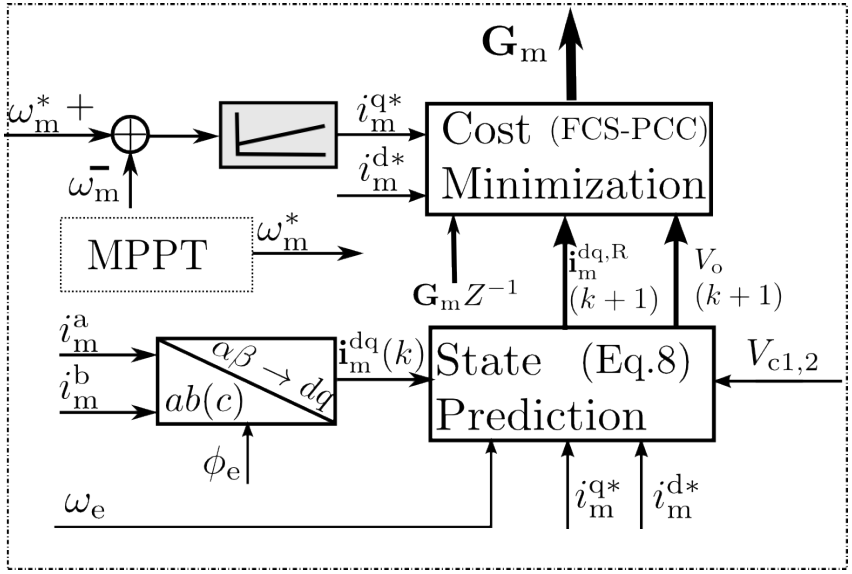

(b)

Fig.: Structure of (a) the classical and (b) the proposed FCS-MPC.

Proposed solution

Against inductance variations:

$$\boldsymbol{x}_\mathrm{m}^{\mathrm{new}}(k) = (1-\lambda)\cdot \boldsymbol{x}_\mathrm{m}^{\mathrm{p}}(k) + \lambda \cdot \boldsymbol{x}_\mathrm{m}^{m}(k),\ \ \lambda \in (0,\,1] \qquad \text{(Eq. 4)}$$

where $\boldsymbol{x}_\mathrm{m}^{\mathrm{p}}$ stands for "predicted" and $\boldsymbol{x}_\mathrm{m}^{m}$ for "measured" values, λ is a tuning factor.

stable ⇔

All roots of $F(z)$ are inside the unit circle

$$\frac{\boldsymbol{x}_\mathrm{m}^{m}(z)}{\boldsymbol{x}_\mathrm{m}^{*}(z)} = \frac{\frac{\hat{L}_\mathrm{m}}{L_\mathrm{m}} z + \left(1-\frac{\hat{L}_\mathrm{m}}{L_\mathrm{m}}\right)\lambda}{\underbrace{\left(z-\left(1-\frac{\hat{L}_\mathrm{m}}{L_\mathrm{m}}\right)\lambda\right)}_{:=F(z)}} \qquad \text{(Eq. 5)}$$

3. Recent works

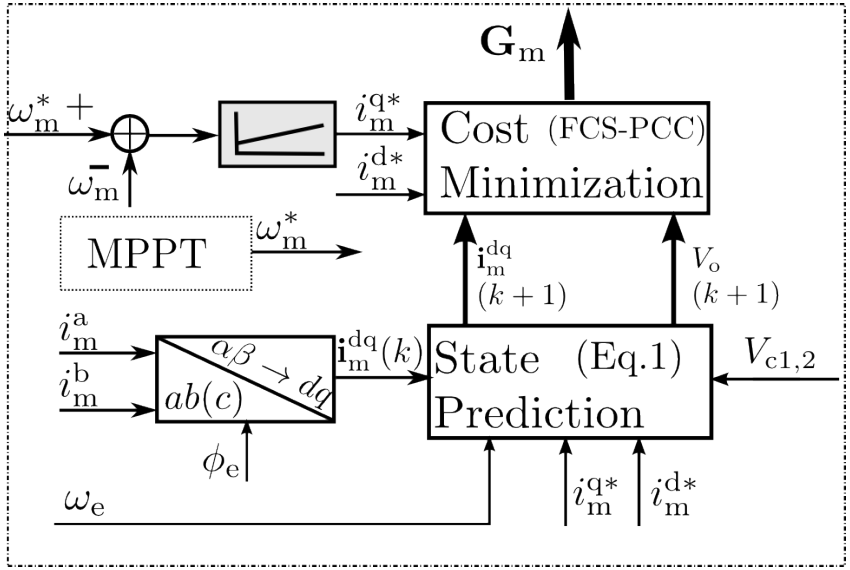

(a)

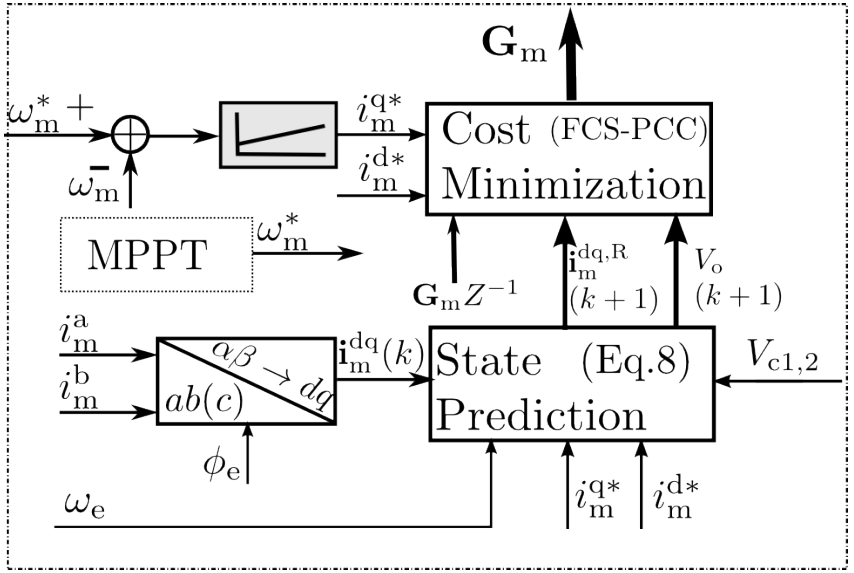

(b)

Fig.: Structure of (a) the classical and (b) the proposed FCS-MPC.

Proposed solution

Against inductance variations:

$$|z| = \left|\left(1 - \frac{\hat{L}_\mathrm{m}}{L_\mathrm{m}}\right)\lambda\right| < 1 \Leftrightarrow 0 < \frac{\hat{L}_\mathrm{m}}{L_\mathrm{m}} < \underbrace{1 + \frac{1}{\lambda}, \quad \text{where,} \quad 0 < \lambda \leq 1}_{:= \kappa_{max} \geq 2} \qquad \text{(Eq. 6)}$$

The safety/stability range of inductance value $\hat{L}_\mathrm{m}$ in the controller is enlarged from the original/conventional solution $(0, 2L_\mathrm{m})$ to $(0, \kappa_{max} \cdot L_\mathrm{m})$.

3. Recent works

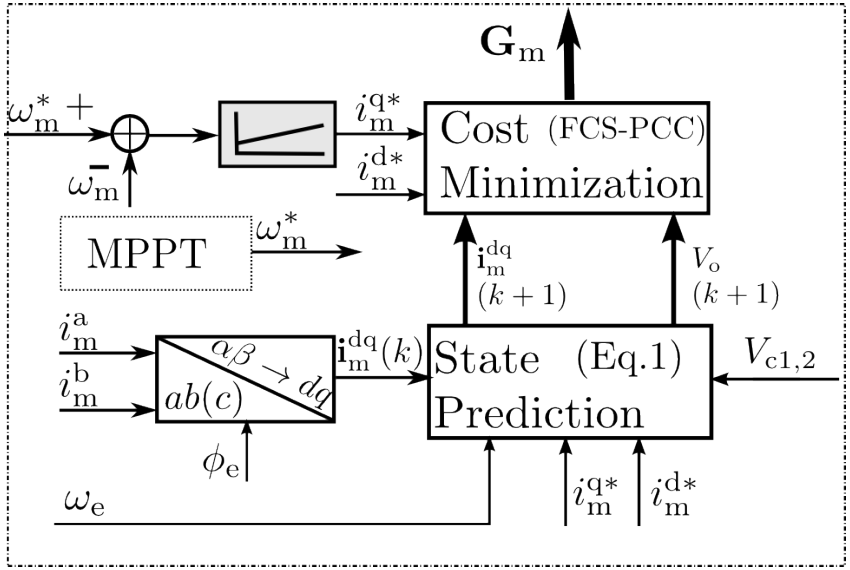

(a)

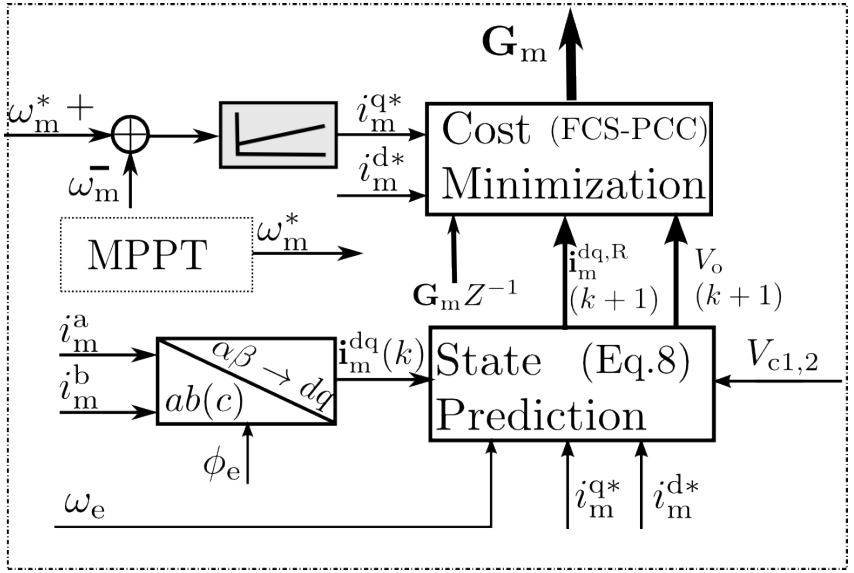

(b)

Fig.: Structure of (a) the classical and (b) the proposed FCS-MPC.

Proposed solution

Against steady-state tracking bias:

$$\boldsymbol{x}_\mathrm{m}^\mathrm{R}(k+1) = \boldsymbol{x}_\mathrm{m}^\mathrm{new}(k+1) + \underbrace{\frac{1-z^{-1}}{1-\alpha_1 z^{-1}}\left(\boldsymbol{x}_\mathrm{m}^*(k) - \boldsymbol{x}_\mathrm{m}^m(k)\right)}_{:=\,\boldsymbol{x}_\mathrm{m}^\mathrm{comp}(k)} \qquad \text{(Eq. 7)}$$

where $x_\mathrm{m}^*(k)$ is the reference value of $x_\mathrm{m}(k)$, α_1 is tuned in a trial and error manner.

3. Recent works

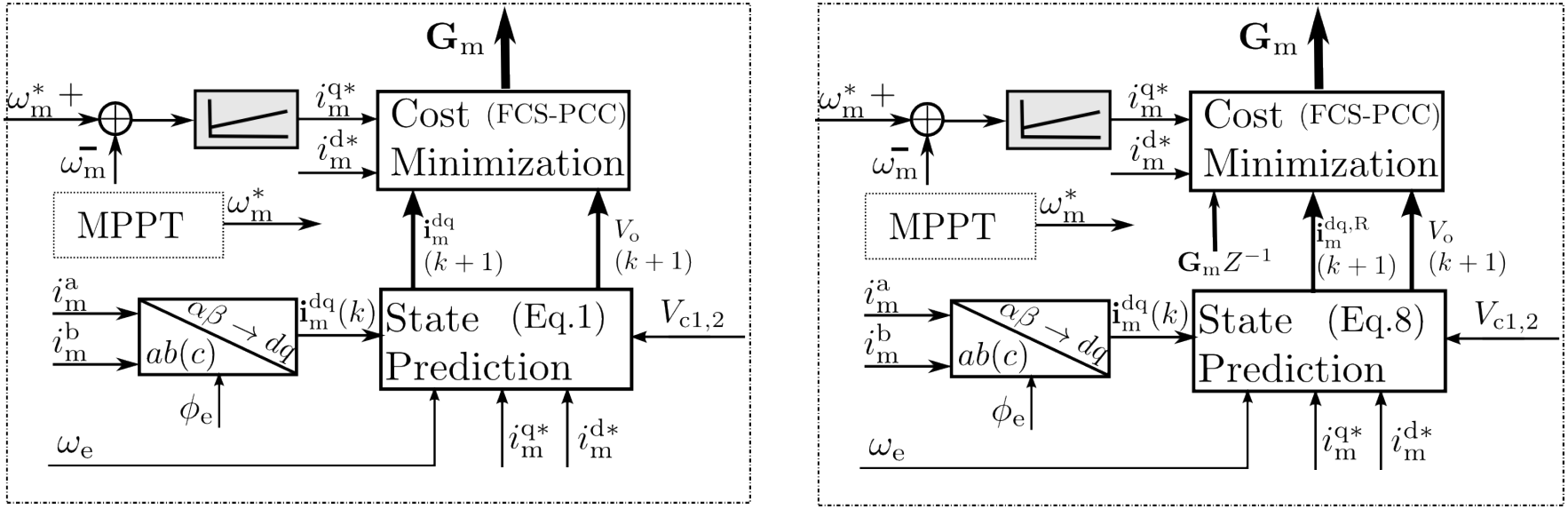

Fig.: Structure of (a) the classical and (b) the proposed FCS-MPC.

Proposed solution

An integration of the state tracking error (between the previously predicted and the currently measured states) can be added into the revised state prediction model.)

$$x_\mathrm{m}^\mathrm{R}(k+1) = x_\mathrm{m}^\mathrm{new}(k+1) + x_\mathrm{m}^\mathrm{comp}(k) \qquad \text{(Eq. 8)}$$

3. Recent works

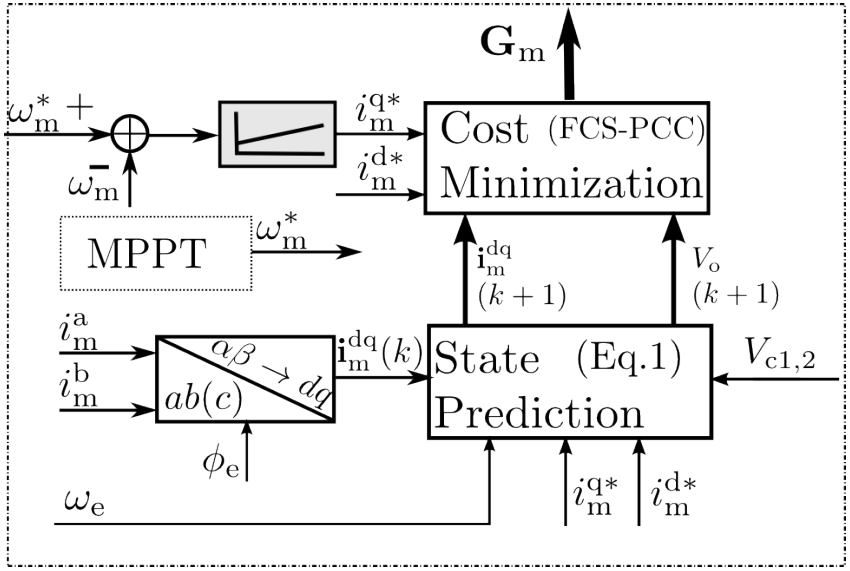

(a)

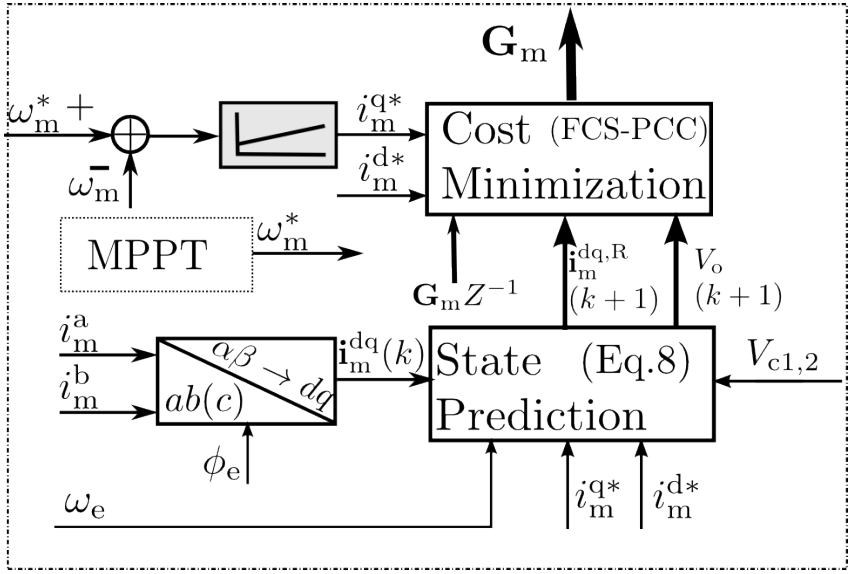

(b)

Fig.: Structure of (a) the classical and (b) the proposed FCS-MPC.

Proposed solution

Against permanent magnet flux linkage variations:

Define $\Delta\psi_\mathrm{pm} := \hat{\psi}_\mathrm{pm} - \psi_\mathrm{pm}$, $\Delta L_\mathrm{s} := \hat{L}_\mathrm{s} - L_\mathrm{s}$

$$i_\mathrm{m}^{\mathrm{q,m}}(k) = \frac{\hat{L}_\mathrm{s}}{L_\mathrm{s}} i_\mathrm{m}^{\mathrm{q,p}}(k) + \frac{\Delta L_\mathrm{s}}{L_\mathrm{s}} T_\mathrm{s}\omega_\mathrm{e}(k-1) i_\mathrm{m}^{\mathrm{d}}(k-1) + \frac{1}{L_\mathrm{s}} T_\mathrm{s}\omega_\mathrm{e}(k-1)\Delta\psi_\mathrm{pm} \qquad \text{(Eq. 9)}$$

In steady state

$$i_\mathrm{m}^{\mathrm{d}}(k-1) = 0, \quad i_\mathrm{m}^{\mathrm{q}}(k) = i_\mathrm{m}^{\mathrm{q}}(k-1)$$

3. Recent works

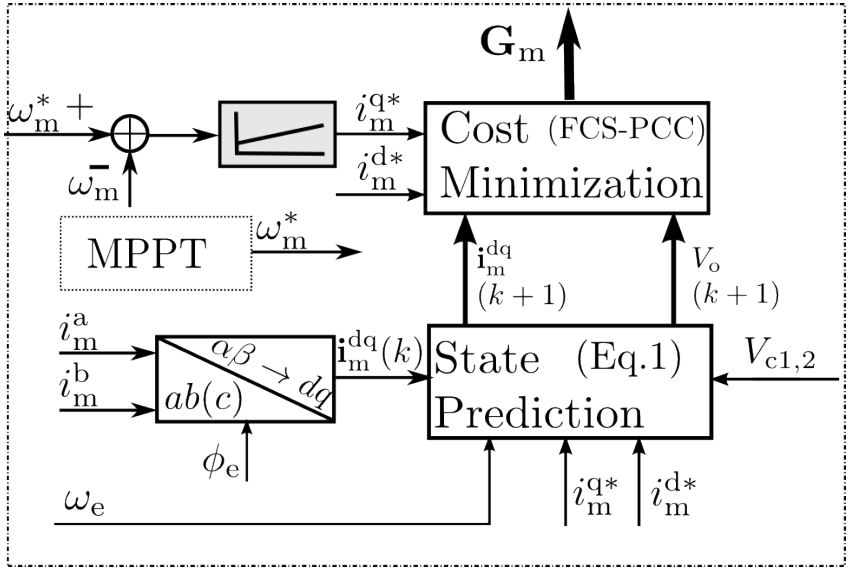

(a)

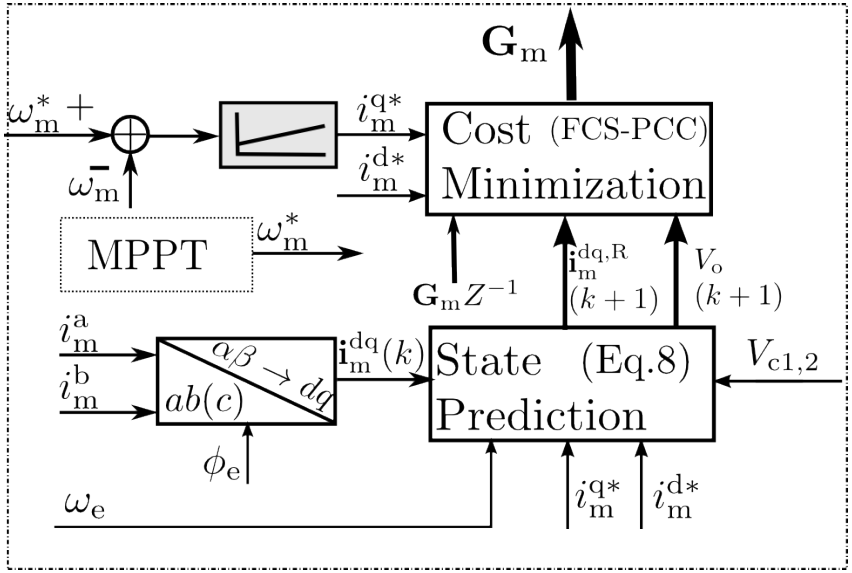

(b)

Fig.: Structure of (a) the classical and (b) the proposed FCS-MPC.

Proposed solution

Against permanent magnet flux linkage variations:

$$i_\mathrm{m}^{\mathrm{q,error}}(k) \coloneqq i_\mathrm{m}^{\mathrm{q,m}}(k) - i_\mathrm{m}^{\mathrm{q,p}}(k) \approx \frac{T_\mathrm{s}\omega_\mathrm{e}(k-1)}{L_\mathrm{s}} \cdot \Delta\psi_\mathrm{pm} \qquad \text{(Eq. 10)}$$

$$\psi_\mathrm{pm}^{\mathrm{new}}(k) \coloneqq \psi_\mathrm{pm}(k) + \underbrace{\alpha_2 \cdot \sum \left(i_\mathrm{m}^{\mathrm{q,error}}(k)\right)}_{\coloneqq \psi_\mathrm{pm}^{\mathrm{comp}}(k)} \qquad \text{(Eq. 11)}$$

where α_2 is tuned in a trial and error manner.

4. Experimental results

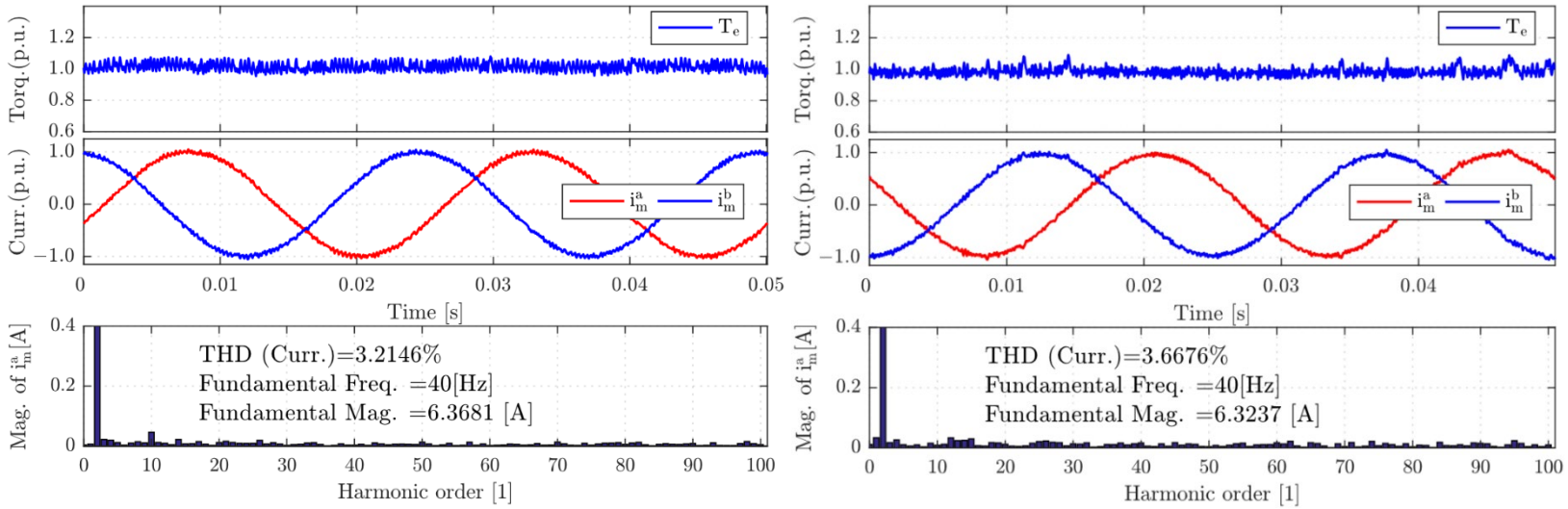

(a) *Robust* FCS-MPC. (b) *Classical* FCS-MPC.

Fig.:[Experimental data:] control performances comparison at ***no parameter variation condition***: For both figures, from up to down are the electromagnetic torque (base value 8.5 [Nm]), stator currents (base value 6.3 [A]) and current spectrum.

4. Experimental results

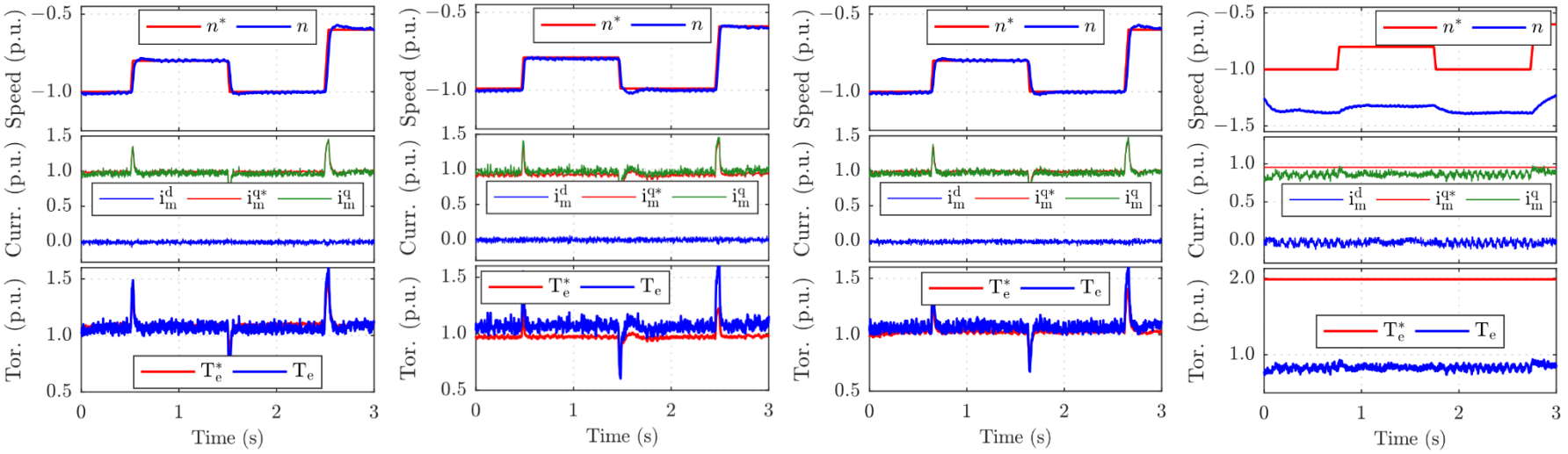

(a) *Robust* FCS-MPC: $0.5\psi_{\mathrm{pm}}$. (b) *Classical* FCS-MPC: $0.5\psi_{\mathrm{pm}}$. (c) *Robust* FCS-MPC: $2\psi_{\mathrm{pm}}$. (d) *Classical* FCS-MPC: $2\psi_{\mathrm{pm}}$.

Fig.: [Experimental data:] performances of the proposed and classical FCS-MPC methods, ***at 50%*** (sub-figure (a) and (b)) ***and 200%*** (sub-figure (c) and (d)) ***of the nominal permanent-magnetic flux conditions*** (ψ_{pm}). For all sub-figures from up to down are the generator speed (base value 1000 [rpm]), stator currents (base value 6.3 [A]) in dq-frame and the electro-magnetic torque (base value 8.5 [Nm]).

4. Experimental results

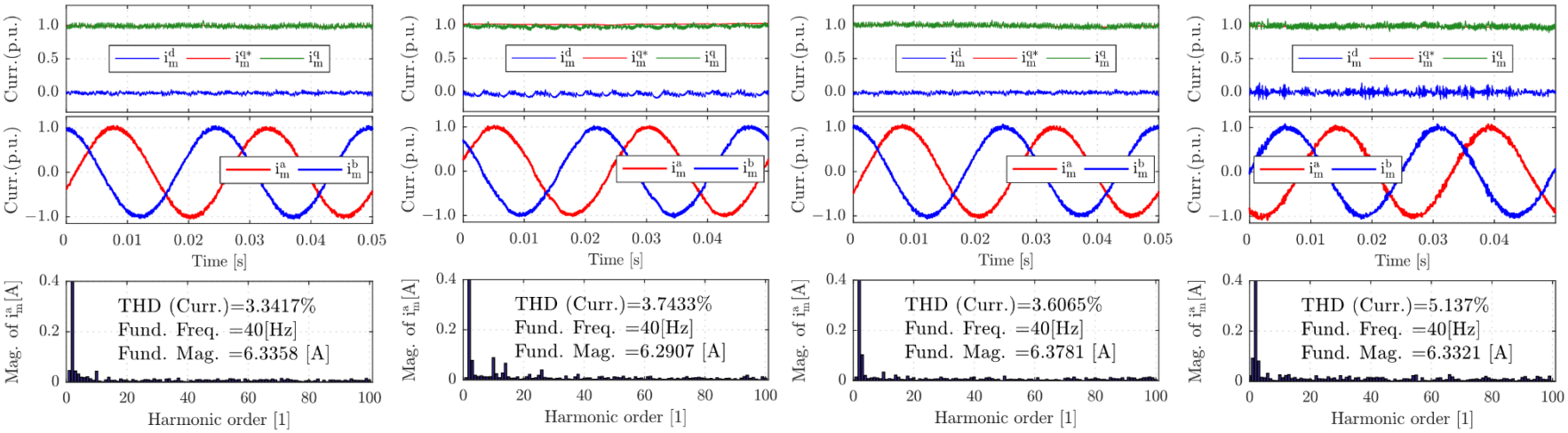

(a) *Robust* MPC (50% L_s). (b) *Classical* MPC (50% L_s). (c) *Robust* MPC (200% L_s). (d) *Classical* MPC (200% L_s).

Fig.: [Experimental data:] performances of the proposed and classical FCS-MPC methods, at ***50% and 200% of the nominal stator inductance condition***. For all sub-figures from up to down are the stator currents (base value 6.3 [A]) in dq and ab(c)-frame and the current spectrum, respectively.

5. Summary

The proposed method is

1. Simple structure and easy to implement;
2. Outperforms the classical FCS-MPC solution, at different scenarios both with and without parameter variations;
3. The proposed solution can be easy extended to other FCS-MPC alternatives (e.g., speed, flux, current control, etc.) with few modifications.

Only a slightly higher FPGA resource usage is required.

5. Summary

1. **Positive features:**
   - Straightforward design procedure
   - Handling of complex & nonlinear dynamics
   - Suitable for MIMO plants
2. **Benefits:**
   - Improved plant performance
   - Reduced engineering effort
   - "Direct" (no modulator) → control structure simplified + fast control dynamics
   - Cost function based → Flexible
3. **Tricky part:**
   Solving the optimization problem → Trade-off between:
   - Control performance
   - Computational complexity/Horizon length

…"mapping from improved system performance aspects to cost savings must be clearly identified and quantified in order to convince industry to adopt novel MPC methods"!!

Thank you for your attention, and glad to know your questions!

Presenter: Zhenbin Zhang
Yongdu Wang

zbz@sdu.edu.cn

Appendix

Parameters	Values
PMSM inductance L_s^d=L_s^q[H]	8×10^{-3}
PMSM resistance R_s [Ω]	1.3
PM Flux ψ_{pm} [Wb]	0.41
DC capacitance $C_1 = C_2$ [F]	1100×10^{-6}
Torque/Current T_e^n/I_m^n [Nm/A]	8.5/6.3
Rated speed n [RPM]	3000
PMSG Pole Pairs N_p[1]	3
Sampling Time T_s [μs]	50
Weights $\gamma_{i_m^d, i_m^q}$, $\gamma_y^{sf,Vo}$ [1]	0.4, 1, 5%, 2%
Parameters $\alpha_{1,2}$, λ [1]	0.02, 0.0043, 0.61

Table: System configuration